



UNIVERSIDADE ESTADUAL DE CAMPINAS – UNICAMP

FACULDADE DE ODONTOLOGIA DE PIRACICABA

THAMARA BELINE

**DESENVOLVIMENTO DE SUPERFÍCIE DE TITÂNIO BIOFUNCIONAL POR MEIO DA OXIDAÇÃO POR
PLASMA ELETROLÍTICO E PLASMA POR DESCARGA INCANDESCENTE PARA APLICAÇÕES
BIOMÉDICAS**

**PRODUCTION OF A BIOFUNCTIONAL TITANIUM SURFACE USING PLASMA ELECTROLYTIC
OXIDATION AND GLOW DISCHARGE PLASMA FOR BIOMEDICAL APPLICATIONS**

**PIRACICABA
2016**

THAMARA BELINE

**DESENVOLVIMENTO DE SUPERFÍCIE DE TITÂNIO BIOFUNCIONAL POR MEIO DA OXIDAÇÃO POR
PLASMA ELETROLÍTICO E PLASMA POR DESCARGA INCANDESCENTE PARA APLICAÇÕES
BIOMÉDICAS**

**PRODUCTION OF A BIOFUNCTIONAL TITANIUM SURFACE USING PLASMA ELECTROLYTIC
OXIDATION AND GLOW DISCHARGE PLASMA FOR BIOMEDICAL APPLICATIONS**

Dissertação apresentada à Faculdade de Odontologia de Piracicaba da Universidade Estadual de Campinas como parte dos requisitos exigidos para a obtenção do título de Mestre em Clínica Odontológica na Área de Prótese Dental.

Dissertation presented to the Piracicaba Dental School of the University of Campinas in partial fulfillment of the requirements for the degree of Master in Dental Clinic in Prosthodontics area.

Orientador: Prof. Dr. Valentim Adelino Ricardo Barão

Este exemplar corresponde à versão final da dissertação defendida por Thamara Beline e orientada pelo Prof. Dr. Valentim Adelino Ricardo Barão.

**PIRACICABA
2016**

Agência(s) de fomento e nº(s) de processo(s): FUNCAMP, 653/13

Ficha catalográfica
Universidade Estadual de Campinas
Biblioteca da Faculdade de Odontologia de Piracicaba
Marilene Girello - CRB 8/6159

B412d Beline, Thamara, 1991-
Desenvolvimento de superfície de titânio biofuncional por meio da oxidação por plasma eletrolítico e plasma por descarga incandescente para aplicações biomédicas / Thamara Beline. – Piracicaba, SP : [s.n.], 2016.

Orientador: Valentim Adelino Ricardo Barão.
Dissertação (mestrado) – Universidade Estadual de Campinas, Faculdade de Odontologia de Piracicaba.

1. Titânio. 2. Corrosão. 3. Implantes dentários. 4. Eletroquímica. 5. Propriedades de superfície. I. Barão, Valentim Adelino Ricardo, 1983-. II. Universidade Estadual de Campinas. Faculdade de Odontologia de Piracicaba. III. Título.

Informações para Biblioteca Digital

Título em outro idioma: Production of biofunctional titanium surface using plasma electrolytic oxidation and glow discharge plasma for biomedical applications

Palavras-chave em inglês:

Titanium

Corrosion

Dental implants

Electrochemistry

Surface properties

Área de concentração: Prótese Dental

Titulação: Mestra em Clínica Odontológica

Banca examinadora:

Valentim Adelino Ricardo Barão [Orientador]

Luís Augusto Sousa Marques da Rocha

Rafael Leonardo Xediek Consani

Data de defesa: 29-02-2016

Programa de Pós-Graduação: Clínica Odontológica



UNIVERSIDADE ESTADUAL DE CAMPINAS
Faculdade de Odontologia de Piracicaba



A Comissão Julgadora dos trabalhos de Defesa de Dissertação de Mestrado, em sessão pública realizada em 29 de Fevereiro de 2016, considerou a candidata THAMARA BELINE aprovada.

PROF. DR. VALENTIM ADELINO RICARDO BARÃO

PROF. DR. LUÍS AUGUSTO SOUSA MARQUES DA ROCHA

PROF. DR. RAFAEL LEONARDO XEDIEK CONSANI

A Ata da defesa com as respectivas assinaturas dos membros encontra-se no processo de vida acadêmica do aluno.

Dedicatória

A Deus

Pelo dom da vida, pela saúde e por minha família. Obrigada, Senhor, por iluminar o meu caminho e por todas as realizações diárias que tem me concedido. Sei que Sua Graça se faz presente em todos os momentos de minha vida e que nunca permite que me falte nada. Obrigada por me dar mais do que mereço.

Aos meus pais Eva e Antônio

Aos meus pais, que abdicaram de muitas de suas vontades para que eu e minha irmã alcançássemos nossos sonhos. A vocês devo tudo o que sou hoje. Obrigada pelo exemplo de simplicidade e humildade e pelo amor incondicional que me deram. Agradeço a Deus todos os dias por ter vocês em minha vida.

A minha irmã Thalita

A minha irmã e melhor amiga Thalita, por todo o carinho e motivação nesta jornada, sempre com alguma palavra de força e coragem para me animar. Obrigada por tudo. Amo você!

Ao meu namorado Lincoln

Ao meu namorado Lincoln, que sempre esteve ao meu lado desde a época do colegial. Com certeza as suas palavras de incentivo foram fundamentais para que eu tivesse mais força para alcançar todos os meus objetivos. Muito obrigada por seu amor, paciência, compreensão e todo o apoio que me deu até hoje. Te amo!

Agradecimentos

Especialmente ao meu orientador **Prof. Dr. Valentim Adelino Ricardo Barão**. Exemplo de professor, pesquisador e pessoa. Sou eternamente grata pela oportunidade de ser sua orientada e crescer pessoal e profissionalmente ao seu lado. Muito obrigada por todo o suporte, paciência, zelo e incentivo. Que Deus continue a abençoar imensamente a sua vida.

A **Universidade Estadual de Campinas – UNICAMP**, na pessoa do Magnífico Reitor, **Prof. Dr. José Tadeu Jorge**, pelo meu mestrado nesta instituição.

A **Faculdade de Odontologia de Piracicaba – UNICAMP**, na pessoa do seu Diretor **Prof. Dr. Guilherme Elias Pessanha Henriques** pela oportunidade da realização do Programa de Pós-Graduação em Clínica Odontológica.

Ao **Laboratório de Plasmas Tecnológicos da Universidade Estadual Paulista “Júlio de Mesquita Filho” – UNESP (Campus de Sorocaba)**, representado pelo **Prof. Dr. Nilson Cristino da Cruz** e pela **Prof. Dra. Elidiane Cipriano Rangel** pela parceria no desenvolvimento deste trabalho.

A **FAEPEX**, pela concessão do auxílio de financiamento do projeto.

A **FAPESP**, pela concessão do auxílio financeiro (Processo 2013/08461-1).

A Coordenadora Geral da Pós-Graduação **Profa. Dra. Cinthia Pereira Machado Tabchoury** e a Coordenadora do Programa de Pós-Graduação em Clínica Odontológica **Profa. Dra. Karina Gonzales Silvério Ruiz**.

Aos docentes **Prof. Dr. Marcelo Ferraz Mesquita**, **Prof. Dr. Rafael Leonardo Xediek Consani**, **Prof. Dr. Mauro Antônio de Arruda Nóbilo**, **Profa. Dra. Altair Del Bel Cury**, **Profa. Dra. Renata Cunha Matheus Rodrigues Garcia**, **Profa. Dra. Célia Rizzati Barbosa** por todo conhecimento compartilhado.

Ao técnico do Laboratório de Plasmas Tecnológicos (UNESP – Sorocaba) **Rafael Parra**, por toda prestatividade na realização das análises necessárias para a realização deste trabalho.

Ao **Prof. Dr. Antônio Pedro Ricomini Filho** pela prontidão, solicitude, atenção e ajuda necessárias no desenvolvimento deste trabalho.

A **Profa. Dra. Isabella da Silva Vieira Marques**, por toda paciência, disponibilidade e ensinamentos transmitidos. Muito obrigada pela sua amizade, prestatividade e dedicação a este trabalho, mesmo nos momentos em que estava mais atarefada. Serei grata eternamente pela oportunidade de conviver e aprender com alguém tão especial.

Aos meus primeiros irmãos de pós-graduação, **Erika Shiguematsu Ogawa**, pelos bons momentos compartilhados, pela grande amizade, pelas comprinhas, pela companhia nas idas ao Galileo e pelos jantares realizados na sua casa e **Adaias Oliveira Matos**, por todas as palavras de conforto nas horas de desespero, pelas idas a Sorocaba e pela amizade sincera. Sem a ajuda

constante de vocês seria muito mais difícil realizar este trabalho. Muito obrigada por toda a solicitude e companheirismo ao longo destes dois anos de pós-graduação. Aos meus irmãos mais novos de pós-graduação, **Jairo Cordeiro**, pelo companheirismo, amizade sincera e prontidão para me ouvir e dar conselhos, **Heloisa Pantaroto**, pela generosidade e alegria e **Halina Berejuk**, pela bondade e simpatia. Muito obrigada por todo carinho e os momentos maravilhosos que compartilhamos até hoje. Com certeza a nossa convivência alegre no laboratório fez pesar muito menos o estresse. Obrigada por terem feito parte desta tão importante etapa da minha vida.

A todos os meus amigos do Laboratório de Prótese Total **Anna Gabriella Camacho Presotto**, **Bruno Zen**, **Claudia Bhering**, **Conrado Caetano**, **Gabriel Meloto**, **Giovana Oliveira**, **Guilherme Machado**, **Moisés Nogueira**, **Júlia Campana**, **Ricardo Caldas**, **Sales Antonio Barbosa Junior** e **Vagner Flávio Reginato**, o meu muito obrigado pela convivência e experiências trocadas.

A Sra. **Eliete A. Ferreira Lima Marim**, secretária do Departamento de Prótese e Periodontia da FOP-UNICAMP, pela atenção e toda gentileza. Ao **Eduardo Pinez (Du)**, técnico do Laboratório de Prótese Total, pelo bom humor e prontidão para ajudar sempre.

A minha amiga **Anne Caroline Ramos**, pela convivência desde a época de graduação. Muito obrigada pela sua sincera amizade e por todo apoio nos momentos bons e nos de tribulação em minha vida. Com certeza ser sua colega de quarto tornou minha vida em Piracicaba muito alegre e feliz.

A minha amiga **Monique Gimenez**. A distância nunca fez com que eu me sentisse longe de você todo esse tempo. Muito obrigada por todas as palavras de incentivo e por sempre estar presente, mesmo que online, todas as vezes que preciso de um ombro amigo.

A todos os meus familiares e amigos, que compreenderam os momentos de ausência durante a realização deste trabalho, obrigada por todo apoio e carinho.

A todos os que fizeram parte, de alguma forma, da minha trajetória no curso de mestrado.

Muito obrigada!

Resumo

Este estudo avaliou o papel dos tratamentos com plasma de oxidação eletrolítica (PEO) e plasma por descarga incandescente (PDI) quanto (i) ao comportamento eletroquímico, (ii) propriedades físicas, químicas e mecânicas e (iii) adsorção de proteínas pelo titânio comercialmente puro (Ticp). Discos de Ticp (15 mm × 2 mm) foram separados em 4 grupos (n=5) em função do tipo de tratamento de superfície. Superfícies polida e jateada com óxido de alumínio (Al₂O₃) foram consideradas controles. Para o ensaio eletroquímico, testes padrões foram conduzidos em saliva artificial (pHs 3,0; 6,5 e 9,0) para simular o ambiente bucal e solução de fluido corpóreo (pH 7,4) para simular o plasma sanguíneo. Testes de caracterização foram realizados, antes e após o ensaio eletroquímico, através da Microscopia Eletrônica de Varredura (MEV), Espectroscopia de Energia Dispersiva (EDS), Microscopia de Força Atômica (AFM), Espectroscopia Fotoeletrônica de Raios-X (XPS), Difratografia de Raios-X (XRD), Perfilometria, Microdureza Vickers e Energia de Superfície. A adsorção de albumina, fibronectina e fibrinogênio foi mensurada através do método do ácido bicinconínico. Os dados foram avaliados por meio da análise de variância e pelo teste Bonferroni ($\alpha=0,05$). Os tratamentos com plasma mostraram melhor comportamento eletroquímico quando comparados aos controles por exibirem maiores valores de resistência à polarização (R_p) e menores valores de capacitância (Q) ($p < 0,05$). A saliva artificial pH 3,0 mostrou os maiores valores de Q para as superfícies polida e jateada ($p < 0,05$). Através das imagens de MEV e AFM foi observado que o grupo PEO mostrou superfície porosa e o grupo PDI exibiu superfície com estrias longitudinais. Na análise do XPS, foram identificados compostos a base de Ca e P na superfície do PEO e a base de Si na superfície do PDI. Superfície com estrutura cristalina foi encontrada no grupo PEO pela análise do XRD. Quanto a rugosidade de superfície, os grupos PEO e jateado apresentaram os maiores valores ($p < 0,05$). O processo corrosivo não alterou os valores de rugosidade de superfície. Os tratamentos com PEO e jateamento aumentaram os valores de microdureza Vickers quando comparados aos demais grupos ($p < 0,05$). Após o processo corrosivo, houve tendência a redução da microdureza em todos os grupos. A energia de superfície inicial foi maior no grupo PDI ($p < 0,05$), o que sugere uma maior hidrofiliabilidade de superfície. Os demais grupos exibiram valores de energia de superfície semelhantes ($p > 0,05$). Após o processo corrosivo, a energia de superfície do PDI reduziu-se significativamente ($p < 0,05$). As superfícies tratadas com PEO e jateamento promoveram altos valores de adsorção de albumina ($p < 0,05$). Os grupos PEO, jateado e PDI aumentaram a adsorção de fibronectina ($p < 0,05$). O grupo PEO mostrou os maiores valores de adsorção para adsorção de fibrinogênio ($p < 0,05$). Assim, conclui-se que as superfícies tratadas com plasma, mostraram maior estabilidade eletroquímica que as superfícies polida e jateada. A saliva artificial em pH ácido

influenciou negativamente o comportamento eletroquímico do Ticp. A presença de Ca, P e Si afetou positivamente a adsorção de proteínas. Os tratamentos com plasma são promissores para implantes biomédicos.

Palavras-chave: Titânio, Corrosão, Implantes dentários, Eletroquímica, Propriedades de superfície, Proteínas.

Abstract

This study aimed to evaluate the role of treatment with plasma electrolytic oxidation (PEO) and glow discharge plasma (GDP) regarding to (i) the electrochemical behavior; (ii) the physical, chemical and mechanical properties and (iii) the protein adsorption of commercially-pure titanium (cp-Ti). Machined and sandblasted surfaces were used as controls. CpTi discs (15 mm × 2 mm) were divided into groups (n = 5) according to the type of surface treatment and electrolytic solution. For the electrochemical assay, standard tests were conducted in artificial saliva (pH 3.0; 6.5 and 9.0) for simulating the oral environment and body fluid solution (pH 7.4) to simulate blood plasma. Characterization tests were performed before and after the electrochemical assay using scanning electron microscopy (SEM), energy dispersive spectroscopy (EDS), X-ray photoelectron spectroscopy (XPS), atomic force microscopy (AFM), X-ray diffraction (XRD), profilometry, Vicker's microhardness and surface energy. The adsorption of albumin, fibronectin and fibrinogen was measured by the bicinchoninic acid method using bovine serum albumin as standard. Data were analyzed using analysis of variance and Bonferroni test ($\alpha=.05$). Treatment with plasma showed better electrochemical behavior than controls, as greater polarization resistance (R_p) values and lower capacitance (Q) values were noted ($p < .05$). The artificial saliva at pH 3.0 showed the highest values of Q than machined and sandblasted surfaces ($p < .05$). SEM and AFM images showed a porous surface for PEO group and longitudinal grooves for GDP group. CaP-based compounds on the surface of PEO were noted via XPS while Si-based compound were noted for GDP surface. XRD showed crystalline structure the PEO group. PEO and sandblasting groups showed the highest roughness values ($p < .05$). The corrosion process did not change the surface roughness values. PEO and sandblasting treatments increased the Vickers hardness values when compared to other groups ($p < .05$). After the corrosion process, a reduction of hardness was noted for all groups. The surface energy of GDP group was the highest ($p < .05$), suggesting an increased of surface hydrophilicity. The other groups exhibited similar surface energy values ($p > .05$). After the corrosion process, GDP energy surface significantly reduced ($p < .05$). Greater albumin adsorption was observed for PEO and sandblasting surfaces ($p < .05$). PEO, sandblasting and GDP groups showed greater fibronectin adsorption ($p < .05$). PEO group showed the highest values for fibrinogen adsorption ($p < .05$). Based on the results, plasma treated samples were able to improve the electrochemical behavior of cpTi when compared to machined and sandblasting surfaces. Acidic saliva reduced the corrosion resistance of cpTi. The presence of Ca, P and Si ions positively affected the protein adsorption results. Plasma is a promising technique to treat biomedical implants.

Key-words: Titanium, Corrosion, Dental implants, Electrochemistry, Surface Properties, Proteins.

Sumário

<i>1- Introdução</i>	11
<i>2- Artigo:</i> Production of a biofunctional titanium surface using plasma electrolytic oxidation and glow discharge plasma for biomedical applications	16
<i>3- Conclusão</i>	57
<i>Referências</i>	58
<i>Anexo 1 - (Copyright)</i>	63

Introdução

O uso de implantes dentários osseointegráveis tem sido difundido para a reabilitação de pacientes parcial ou totalmente edêntulos (Schropp *et al.*, 2014). O titânio comercialmente puro (Ticp) é utilizado atualmente, com alto índice de sucesso em grande número de sistemas de implantes (Bassi *et al.*, 2013). O Ticp apresenta forte ligação com moléculas de água ou ar da atmosfera, o que promove a imediata formação da camada de óxido de titânio (TiO₂) na superfície desse metal (Gupta *et al.*, 2007). Esta propriedade fornece aos implantes a energia de superfície necessária para osseointegração, biocompatibilidade, resistência mecânica (Cortada *et al.*, 2000; Mabboux *et al.*, 2004; Schiff *et al.*, 2002; Vieira *et al.*, 2006) e resistência à corrosão (Souza *et al.*, 2015).

Entretanto, estudos recentes mostraram que o titânio (Ti) pode se degradar quando em contato com substâncias químicas como ácido, flúor e saliva (Barão *et al.*, 2012; Correa *et al.*, 2009; Joska *et al.*, 2010; Nikolopoulou, 2006; Vieira *et al.*, 2006). O processo de corrosão pode afetar a biocompatibilidade e função mecânica dos implantes dentários e possivelmente levar à falha no tratamento (Nikolopoulou, 2006; Messer *et al.*, 2010). A corrente elétrica anormal produzida durante o processo corrosivo pode converter o implante dentário em um eletrodo, e o impacto negativo para o tecido periimplantar, devido a corrente elétrica anormal, pode ser uma causa adicional para a falha dos implantes dentários. Os sinais elétricos alterados podem ainda afetar o desenvolvimento e o reparo ósseo, o que teria implicação direta no processo de osseointegração dos implantes (Gittens *et al.*, 2011). Clinicamente, materiais de implantes dentários que apresentem maior resistência à corrosão podem contribuir com uma melhor interface de osseointegração do implante ao tecido ósseo (Huang *et al.*, 2005; Kotsovilis *et al.*, 2006; Sawase *et al.*, 2007).

No ambiente bucal, os implantes são expostos a vários fatores adversos de origem mecânica (mastigação), físico-química (saliva, flúor, pH e temperatura) e microbiológica (biofilme e seus metabólitos) o que pode ser considerado um complexo processo de degradação contínua (Nakagawa *et al.*, 2002; Souza *et al.*, 2013). A presença de eletrólitos na saliva pode criar mais danos ao induzir fendas de corrosão na interface implante/corona (Nikolopoulou, 2006). O pH da saliva varia nas áreas ao redor dos implantes. Alimentos como o leite, seus derivados e castanhas podem alcalinizar o pH salivar (Murrell *et al.*, 2010). Além disso, pacientes com uremia exibem maior concentração de ureia na cavidade bucal, o que pode implicar no aumento do pH salivar (Edgard *et al.*, 2010). Entretanto, várias situações podem acidificar o pH salivar como infecções, determinados alimentos (alimentos açucarados, em conserva, azedos, frutas, sucos e refrigerantes – pH variando de 2,5 a 3,5), enxaguatórios bucais (Dong *et al.*, 1999; Gregory-Head *et al.*, 2000; Murrell *et al.*, 2010), fumo, doenças crônicas/sistêmicas e medicamentos, o que pode contribuir para a corrosão dos implantes

dentários (Correa *et al.*, 2009; Nikolopoulou, 2006; Vieira *et al.*, 2006). Barão *et al.* (2012) investigaram a influência de diferentes níveis de pH da saliva (3; 6,5 e 9) sobre o comportamento corrosivo do Ticp e da liga Ti-6Al-4V. O pH da saliva afetou consideravelmente o comportamento corrosivo dos dois tipos de Ti. Em pH baixo, foi observada a aceleração de troca iônica entre Ti e saliva, e redução da resistência da superfície do Ti contra a corrosão e o comportamento corrosivo foi semelhante para o Ticp e a liga Ti-6Al-4V.

Os produtos da corrosão podem induzir uma reação inflamatória que pode provocar a liberação de mediadores inflamatórios a partir de macrófagos, contribuindo no processo de reabsorção óssea (Nikolopoulou, 2006). Guindy *et al.* (2004) observaram a falha de implantes dentários de Ti após a osseointegração como consequência da corrosão (fendas de corrosão) na interface implante-coroa. O tecido ósseo coletado ao redor do implante mostrou incorporação de íons metálicos como resultado desse processo corrosivo. Devido a diminuição do fluxo de oxigênio e presença de metabólitos bacterianos, houve redução do pH na região da interface coroa/implante, o que tornou esta área mais susceptível ao processo corrosivo. Olmedo *et al.* (2010) relataram dois casos clínicos de lesões reacionais na mucosa periimplantar, o que indicava tratar-se de partículas de Ti liberadas para os tecidos adjacentes, suscitando na corrosão da superfície dos implantes osseointegrados. Estudos na mucosa periimplantar (Flatebo *et al.*, 2011; Matthew *et al.*, 1996; Olmedo *et al.*, 2002; Olmedo *et al.*, 2010; Olmedo *et al.*, 2012) comprovaram a presença de partículas de Ti distribuídas na região periimplantar e em órgãos de metabolização como rim, fígado, baço e linfonodos próximos aos implantes ou não (Jacobs *et al.*, 1998; Urban *et al.*, 2000). Com o objetivo de acelerar o processo de osseointegração dos implantes, diversos métodos têm sido desenvolvidos para modificar a superfície do Ti, como o jateamento, tratamento ácido, anodização, ou recobrimentos com cálcio e fósforo (Hanawa, 2011). A camada de proteínas proveniente do plasma sanguíneo ou outra solução fisiológica, que é adsorvida na superfície do implante, media a interação com as células e determina a resposta celular ao biomaterial (Davies, 2003). A alteração das propriedades físicas e químicas do Ti melhora a adsorção de proteínas e a adesão celular (Chang *et al.*, 2013). Li *et al.* (2010) estudaram o efeito do tratamento com ácido hidrófluorídrico na ancoragem mecânica e osseointegração de implantes com superfície jateada. O ataque ácido após o jateamento melhorou a osseointegração e ancoragem mecânica do Ti. No entanto, o processo de jateamento afetou negativamente as propriedades mecânicas da superfície do Ti.

Técnicas de modificação de superfície têm sido estudadas para se obter superfícies sem submeter o Ti a elevadas temperaturas, para que as propriedades físico químicas do metal não sejam alteradas. O tratamento de superfície denominado Oxidação por Plasma Eletrolítico (PEO) é uma técnica capaz de melhorar a bioatividade da superfície através da incorporação de espécies iônicas como cálcio (Ca) e fósforo (P), elementos que estão presentes nos ossos (Alves *et al.* 2013; Felgueiras

et al. 2014). Os revestimentos através da técnica de oxidação por plasma eletrolítico melhoram a resistência ao desgaste e à corrosão, promovendo proteção térmica e boa adesão interfacial com o Ti e suas ligas. (Rafieerad *et al.*, 2015). O tratamento de superfície através do PEO promove não só a criação de microporos, como também o maior contato implante-osso, acelerando a formação óssea e a osseointegração (Souza *et al.*, 2015).

Outra técnica de tratamento de superfície estudada é a do Plasma por Descarga Incandescente (PDI) que pode ser definida como um gás com alto grau de ionização e partículas com carga que apresentam múltiplas interações, sendo macroscopicamente neutro, para modificar a superfície de biomateriais à temperatura ambiente e baixa pressão atmosférica (Aronsson *et al.*, 1997; Chang *et al.*, 2013; Czarnowska *et al.*, 2000; Sharma *et al.*, 1991). Este tratamento rompe as ligações covalentes na superfície do material, sendo realizado em uma mistura gasosa com elétrons de alta energia, íons, fótons de raios ultravioleta e de espécies reativas com energia neutras. Recentemente, tem sido utilizado para tratamento de superfície de Ti devido a ação de limpeza altamente eficiente e propriedade de desinfecção/esterilização (Chang *et al.*, 2013; Kibayashi *et al.*, 2005). O PDI além de ser um método eficaz e econômico, tem o atrativo de promover tratamento com profundidade limitada a poucos nanômetros da superfície, dessa maneira consegue-se modificar a superfície e ao mesmo tempo manter as propriedades de massa e função do metal. Adicionalmente, a temperatura do gás empregada na técnica pode permanecer tão baixa quanto a temperatura ambiente (Hauser *et al.*, 2009; Bazaka *et al.*, 2011).

Pesquisas anteriores mostraram que esta técnica de PDI tem sido utilizada para a criação de uma série de grupos funcionais, aumentando a molhabilidade da superfície e aplicação de proteínas funcionais para as superfícies de Ti. Chang *et al.* (2013) utilizaram a tecnologia de PDI realizando incorporação de proteínas à superfície de Ti, incluindo a albumina, colágeno tipo I e fibronectina, para melhorar a biocompatibilidade da superfície do Ti. Sabe-se que a adesão das células ao substrato depende fortemente da fibronectina, uma vez que essa proteína é importante no processo do crescimento celular, migração e diferenciação. Como resultado do trabalho, o tratamento por PDI combinado com enxerto de fibronectina aumentou a hidrofiliabilidade e rugosidade da superfície dos discos de Ti, o que pode atribuir a afinidade de adesão celular, migração, proliferação e diferenciação. O PDI melhora o processo de osseointegração tanto *in vitro* quanto *in vivo*, aumentando o número de trabéculas ósseas ligadas ao implante (MacDonald *et al.*, 2013; Rapuano *et al.*, 2012).

O aumento da molhabilidade pelos materiais de implantes pode melhorar a absorção de proteínas, aumentando a adesão e proliferação de osteoblastos (Arima & Iwata, 2007; Kilpadi *et al.*, 2001). Além disso, uma vez que as proteínas são absorvidas na superfície dos implantes, sítios de ligação celular estarão disponíveis para as integrinas (Bergkvist *et al.*, 2003). A superfície também

influencia nos eventos biológicos após a inserção do implante. Superfícies micro/nanoestruturadas aumentam a absorção de proteínas e consequente adesão de osteoblastos (Gao *et al.*, 2009; Yun *et al.*, 2010).

O hexametildisiloxano (HMDSO) é um monômero organo-silício de interesse devido a sua alta taxa de deposição e a habilidade de controlar a estrutura e propriedade de filme formado na superfície pela variação das condições de deposição (Lee & Lee, 1998; Yoshinari *et al.*, 2004). A incorporação de O₂ durante o processo de deposição do HMDSO melhora as propriedades tribológicas do filme (Lopes *et al.*, 2012). Este tratamento promove alterações na molhabilidade da superfície, propiciando alterações na adsorção de proteínas e no comportamento das células (Hao & Lawrence, 2004; Janocha *et al.*, 2001), entretanto o efeito desse tratamento no processo corrosivo do Ti é limitado. Vargas *et al.* (1992) observaram que o tratamento com PDI com gás argônio reduziu a corrosão da superfície de implantes de Ti-6Al-4V após imersão em solução salina (pH 3) por 2 a 12 semanas. A incorporação de nitrogênio por meio do PDI manteve as propriedades eletroquímicas das ligas Ti-6Al-4V e Ti-5Al-2.5Fe em solução de Hank (Bordji *et al.*, 1996).

Os tratamentos de superfícies, de modo geral, têm melhorado a resposta biológica e o processo de osseointegração dos implantes dentários quando comparados aos de superfícies usinadas (Albrektsson & Wennerberg, 2004). Porém, quando submetidos a esses tratamentos, o Ti e suas ligas podem sofrer mudanças em sua composição, o que pode aumentar potencialmente a liberação de íons para o meio biológico (Coelho *et al.*, 2009). O acúmulo de íons metálicos nos tecidos periimplantares pode resultar em efeitos celulares e teciduais adversos (Eisenbarth *et al.*, 2004; Hanawa *et al.*, 1992). A estabilidade eletroquímica da superfície dos implantes é importante para manutenção da saúde peri-implantar e longevidade do tratamento. Entretanto, o papel desses novos tratamentos de superfície no comportamento corrosivo do Ti é muito limitado. Sabe-se ainda que o uso do plasma para tratamento de superfície de biomateriais é considerado um “*hot topic*” nas áreas de engenharia de materiais e engenharia biomédica, possibilitando o desenvolvimento de materiais com maior biocompatibilidade e longevidade.

Considerando-se que o papel dos diferentes tratamentos de superfície no comportamento corrosivo do Ti é discutível e sabendo-se que a maioria dos estudos realizados na área de corrosão são voltados à ortopedia médica e pouca atenção tem sido dada ao comportamento corrosivo do Ti no ambiente oral, os objetivos do presente estudo são (i) avaliar o papel dos tratamentos com plasma de oxidação eletrolítica e plasma descarga incandescente no comportamento eletroquímico do Ticp em saliva artificial (pHs 3,0, 6,5 e 9,0) e solução de fluido corpóreo; (ii) caracterizar as propriedades físicas, químicas e mecânicas dos tratamentos de superfície propostos e (iii) investigar a adsorção de proteínas do soro sanguíneo nas superfícies modificadas.

As hipóteses do presente estudo foram: (i) os tratamentos com plasma melhorariam a estabilidade eletroquímica e o meio ácido reduziria a resistência à corrosão do Ticp; (ii) os tratamentos propostos modificariam as propriedades físicas, químicas e mecânicas do Ticp; (iii) a adsorção de proteínas nas superfícies tratadas com PEO e PDI seria maior.

Assim, os resultados desse estudo fornecem dados sobre o efeito de novos tratamentos de superfícies na estabilidade eletroquímica do Ticp na cavidade oral, o que poderá auxiliar no desenvolvimento de superfícies de implantes dentários com menor potencial corrosivo e consequente maior longevidade do tratamento.

***Artigo:* Production of a biofunctional titanium surface using plasma electrolytic oxidation and glow discharge plasma for biomedical applications**

Running title: Biofunctional titanium surface

Running authors: Beline et al.

Thamara Beline^{1,a)}, Isabella S. V. Marques^{1,b)}, Adaias O. Matos^{1,c)}, Erika S. Ogawa^{1,d)}, Antônio P. Ricomini-Filho^{2,e)}, Elidiane C. Rangel^{3,f)}, Nilson C. da Cruz^{3,g)}, Cortino Sukotjo^{4,h)}, Mathew T. Mathew^{5,i)}, Richard Landers^{6,j)}, Rafael L. X. Consani^{1,k)}, Marcelo F. Mesquita^{1,l)}, Valentim A. R. Barão^{1,m)}

¹ Department of Prosthodontics and Periodontology, Piracicaba Dental School, University of Campinas (UNICAMP), Av Limeira, 901, Piracicaba, São Paulo 13414-903, Brazil

² Department of Physiological Science, Piracicaba Dental School, University of Campinas (UNICAMP), Av Limeira, 901, Piracicaba, São Paulo 13414-903, Brazil

³ Laboratory of Technological Plasmas, Engineering College, Univ Estadual Paulista (UNESP), Av Três de Março, 511, Sorocaba, São Paulo 18087-180, Brazil

⁴ Department of Restorative Dentistry, University of Illinois at Chicago, College of Dentistry, 801 S Paulina, Chicago, Illinois 60612

⁵ Department of Orthopedic Surgery, Rush University Medical Center, 1611 W Harrison, Chicago, Illinois 60612

⁶ Institute of Physics Gleb Wataghin, University of Campinas (UNICAMP), Cidade Universitária Zeferino Vaz, Barão Geraldo, Campinas, São Paulo 13083-859, Brazil

a) Electronic mail: thamara.beline@gmail.com

b) Electronic mail: isabellamarques@gmail.com

- c) Electronic mail: adaiasmatos@hotmail.com
- d) Electronic mail: erika.s.ogawa@hotmail.com
- e) Electronic mail: pedroricomini@gmail.com
- f) Electronic mail: elidiane@sorocaba.unesp.br
- g) Electronic mail: nilson@sorocaba.unesp.br
- h) Electronic mail: csukotjo@uic.edu
- i) Electronic mail: mathew_t_mathew@rush.edu
- j) Electronic mail: landers@ifi.unicamp.br
- k) Electronic mail: rconsani@fop.unicamp.br
- l) Electronic mail: mesquita@fop.unicamp.br
- m) Author to whom correspondence should be addressed. Electronic mail: vbarao@unicamp.br

Reprinted with permission from Thamara Beline, Isabella S. V. Marques, Adaias O. Matos, Erika S. Ogawa, Antônio P. Ricomini-Filho, Elidiane C. Rangel, Nilson C. da Cruz, Cortino Sukotjo, Mathew T. Mathew, Richard Landers, Rafael L. X. Consani, Marcelo F. Mesquita, Valentim A. R. Barão, *Biointerphases*, **11**, 011013, <http://dx.doi.org/10.1116/1.4944061>, Copyright 2016, American Vacuum Society.

In this study, we tested the hypotheses that plasma electrolytic oxidation (PEO) and glow-discharge plasma (GDP) would improve the electrochemical, physical, chemical, and mechanical properties of commercially pure titanium (cpTi), and that blood protein adsorption on plasma-treated surfaces would increase. Machined and sandblasted surfaces were used as controls. Standard electrochemical tests were conducted in artificial saliva (pHs of 3.0, 6.5, and 9.0) and simulated body fluid. Surfaces were characterized by scanning electron microscopy, energy-dispersive spectroscopy, x-ray photoelectron spectroscopy, atomic force microscopy, x-ray diffraction, profilometry, Vickers microhardness, and surface energy. For biological assay, the adsorption of blood serum proteins (*i.e.*, albumin, fibrinogen, and fibronectin) was tested. Higher values of polarization resistance and lower values of capacitance were noted for the PEO and GDP groups ($p < 0.05$). Acidic artificial saliva reduced the corrosion resistance of cpTi ($p < 0.05$). PEO and GDP treatments improved the surface properties by enrichment of the surface chemistry with bioactive elements and increased surface energy. PEO produced a porous oxide layer (5- μm thickness), while GDP created a very thin oxide layer (0.76- μm thickness). For the PEO group, we noted rutile and anatase crystalline structures that may be responsible for the corrosion barrier improvement and increased microhardness values. Plasma treatments were able to enhance the surface properties and electrochemical stability of titanium, while increasing protein adsorption levels.

Key words: Electrochemistry, Corrosion, Electrochemical Impedance Spectroscopy, Titanium Dioxide, Dental Implant, Blood Proteins.

I. INTRODUCTION

Dental implants have been widely used for the rehabilitation of partially or completely edentulous patients.¹ Commercially pure titanium (cpTi) is mainly used because it has been shown to have a high success rate and clinical longevity in a large number of implant systems.² The cpTi reacts with molecules of water or air from the atmosphere, which promotes immediate formation of a titanium oxide layer (TiO₂) on the metal surface.³ This property provides the surface energy required for implant osseointegration, biocompatibility, mechanical strength,⁴ and corrosion resistance.⁵

In the oral environment, implants are exposed to various adverse factors of mechanical (mastication), chemical (saliva, fluoride, pH, and temperature), and microbiological (biofilm) origins, which can be considered a complex process of continuing degradation.⁶ Barao *et al.*⁷ investigated the influence of different pH levels of saliva (3, 6.5, and 9) on the corrosive behavior of cpTi and a Ti-6Al-4V alloy. The acidic saliva significantly reduced the corrosion resistance of both Ti types. At low pH, titanium released more ions into the saliva, which reduced its corrosion resistance.^{7, 8} Corrosion products can induce an inflammatory reaction, which can cause the release of inflammatory mediators from macrophages, contributing to bone resorption.⁹ Studies in the peri-implant mucosa¹⁰ confirmed the presence of Ti particles distributed in the peri-implant region and metabolic organs such as the kidney, liver, spleen, and lymph nodes both near to and far from the implant site.¹¹

For acceleration of the osseointegration process of dental implant surfaces, several methods have been developed to modify Ti surfaces, such as sandblasting, acid-etching, anodization, or calcium phosphate coatings.¹² The modification of the physical and chemical properties of Ti surfaces facilitates the improvement of protein adsorption and cell adhesion.¹³ A layer of proteins that adsorb to the implant surface from plasma or other physiological fluids mediates the interaction with cells and determines the cellular response to the biomaterial.¹⁴ Changes in the surface topography and composition can affect the protein adsorption characteristics.¹⁵ Li *et al.*¹⁶ studied the effect of acid-etching using hydrofluoric acid on the mechanical anchorage and osseointegration of sandblasted Ti

implants. The acid attack after blasting improved the osseointegration and mechanical stability of Ti. However, the blasting process caused the mechanical properties of the Ti surface to deteriorate.

Surface modification techniques have been studied to obtain surfaces without subjecting Ti to treatments at elevated temperatures, preventing changes in the physical-chemical properties of the metal. The surface treatment designated Plasma Electrolytic Oxidation (PEO) is a technique capable of enhancing surface bioactivity by the incorporation of ionic species, such as calcium (Ca) and phosphorus (P) elements present in the bone.¹⁷ PEO coatings improved wear and corrosion resistance, promoted thermal protection, and showed good interfacial adhesion in Ti and its alloys.¹⁸ Surfaces treated with PEO not only promoted the creation of micropores, but also accelerated bone formation, promoting osseointegration and improving implant-bone contact.¹⁹ Another surface treatment methodology that has been recently applied is called glow-discharge plasma (GDP), defined as a gas with a high degree of ionization and charged particles that have multiple interactions, being macroscopically neutral, to modify the surfaces of biomaterials at room temperature and low pressure.¹³ Besides being an efficient and economical method, GDP is attractive for promoting treatment with depth limited to a few nanometers of the surface. Therefore, it is possible to modify a surface while maintaining its mass properties and metal function.²⁰ Additionally, the temperature of the gas used in this technique can remain as low as room temperature.²¹ This treatment causes changes in surface wetting, providing changes in protein adsorption and cell behavior.²²

In general, surface treatments have improved biological response and the osseointegration process of dental implants when compared with machined surfaces.²³ However, when subjected to these treatments, Ti and its alloys may undergo changes in their composition, which can potentially increase the release of ions to the biological environment.²⁴ The accumulation of metal ions in the peri-implant tissues may result in adverse cellular and tissue effects.²⁵ The electrochemical stability of the implant surface is important for the maintenance of peri-implant health and the longevity of treatment. The influence of surface treatments on the corrosion behavior of Ti remains controversial.

Aparicio *et al.*²⁶ showed that the blasting particles of aluminum (Al) and silicon carbide (SiC) at the surface increased the corrosion resistance of cpTi. Conversely, Barranco *et al.*²⁷ observed that the blasted surface of a Ti6Al4V alloy was highly reactive due to the impact of alumina particles on the substrate surface, exhibiting an increased susceptibility to corrosion. Similar results were obtained by Szesz *et al.*,²⁸ wherein the blasting process with Al₂O₃ caused the electrochemical properties of cpTi to deteriorate. Zhou *et al.*²⁹ found that deposition of hydroxyapatite (HA) by sputtering reduced the corrosive resistance of cpTi in Hanks' solution. In a similar study, Coelho *et al.*²⁴ concluded that HA deposition by sputtering does not alter the corrosive properties of the alloy Ti-6Al-4V. However, Kwok *et al.*³⁰ demonstrated that the HA coating made by electrophoretic deposition has increased corrosion resistance of the Ti-6Al-4V alloy when compared with that of an untreated surface. Vargas *et al.*³¹ found that treatment with argon gas GDP impaired the corrosion stability of a Ti-6Al-4V implant after immersion in saline solution (pH 3). The incorporation of nitrogen through the GDP maintained electrochemical properties of Ti-6Al-4V and Ti-5Al-2.5Fe alloys in Hanks' solution.³²

As observed, the role of different surface treatments in the corrosion behavior of Ti remains controversial. Additionally, most corrosion studies have focused on medical orthopedics implants, and little attention has been paid to the corrosion behavior of Ti in the oral environment. Therefore, the aims of this study were: (i) to evaluate the role of PEO and GDP treatments in the electrochemical behavior of cpTi in artificial saliva (pHs 3.0, 6.5, and 9.0) and simulated body fluid (SBF); (ii) to characterize the physical, chemical, and mechanical properties of the Ti coatings; and (iii) to investigate the adsorption of blood proteins onto the modified surfaces.

II. EXPERIMENTAL

A. Experimental design

CpTi discs were randomly divided into four groups according to surface treatments: machined (control), sandblasted (control), PEO, and GDP. The electrochemical stability of such surfaces was tested in artificial saliva at different pHs (3.0, 6.5, and 9.0) and SBF. The following dependent variables were obtained: open circuit potential (OCP), polarization resistance (R_p), constant phase element (CPE), corrosion potential (E_{corr}), corrosion current density (I_{corr}), and passivation current density (I_{pass}). Surfaces were characterized via scanning electron microscopy (SEM), energy-dispersive spectroscopy (EDS), x-ray photoelectron spectroscopy (XPS), atomic force microscopy (AFM), x-ray diffraction (XRD), profilometry, Vickers' microhardness, and surface energy. For biological assay, the adsorption of blood serum proteins (*i.e.*, albumin, fibrinogen, and fibronectin) was tested (Fig. 1).

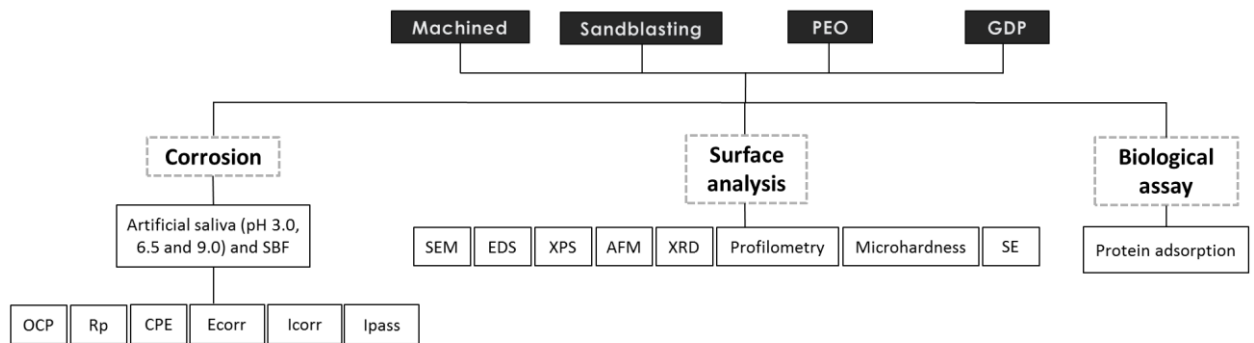


FIG. 1. Schematic diagram of the experimental design.

B. Surface treatments

CpTi discs (American Society for Testing and Materials—Grade II) (MacMaster Carr), 15 mm in diameter and 2 mm in thickness, were used. The chemical composition (in wt. %) of cpTi was Ti (99.7), O₂ (0.16), N₂ (0.004), C (0.006), H₂ (0.0019), and Fe (0.12).³³ Discs were polished with sequential SiC grinding paper (#320, #400, and #600) (CarbiMet 2, Buehler) by means of an automatic polisher (EcoMet/AutoMet 250 Pro, Buehler) at 250 rpm for 1 min with each abrasive paper.

1. Machined and sandblasted (control groups)

In this study, two control groups were considered: a polished (machined) surface as described above and a sandblasted, large-grit, acid-etched surface (sandblasted). The second control group was used to compare the proposed surface treatment with a well-established surface treatment.

For the sandblasted group, cpTi discs were sandblasted with 150 μm Al_2O_3 particles (Polidental Indústria Comércio Ltd) at 50 mm of distance and a 90° angle with pressure of 0.45 MPa for 30 s.³⁴ Then, the discs were washed in an ultrasonic bath with distilled water for 15 min and dried at room temperature. Subsequently, disc surfaces were chemically treated with a solution containing 0.1 mol/L of HCl and 8.8 mol/L of H_2O_2 at 80°C for 20 min, washed in distilled water, oven-dried at 50°C for 12 h, heated with air at 400°C for 1 h, and cooled in an electric oven. Finally, they were washed in distilled water and vacuum-dried.³⁵

2. Plasma electrolytic oxidation (PEO)

Prior to PEO treatment, the discs were washed and degreased with acetone, alcohol, and distilled water for 10 min in an ultrasonic bath and then air-dried. The PEO treatment has been previously described.³⁶ Briefly, a pulsed DC power supply (Plasma Technology Ltd.) was used. A steel tank with a cooling system was used as the cathode, and the cpTi disc was used as the anode. The treatment was performed with an electrolytic solution that was prepared by the dissolution of 0.3 M of calcium acetate [$\text{Ca} (\text{CH}_3\text{CO}_2)_2$] (Sigma–Aldrich) and 0.02 M of glycerophosphate disodium ($\text{C}_3\text{H}_7\text{Na}_2\text{O}_6\text{P}$) (Sigma–Aldrich) in distilled water. The voltage, frequency, and duty cycle were set at 290 V, 250 Hz, and 60%, respectively. The treatment was conducted for 10 min, and the temperature of the electrolyte was maintained at 20°C. Afterwards, the cpTi discs were washed with deionized water and air-dried.

3. Glow-discharge plasma (GDP)

The cpTi discs were ultrasonically washed and degreased in distilled water and detergent (Det limp 32, Chemco) for 15 min, rinsed in water, washed with acetone for 15 min, and then air-dried. GDP treatment was performed inside a custom-made glass reactor fully described elsewhere.³⁷ Discs were sputter-cleaned for 600 s in a plasma atmosphere composed of 50% argon and 50% H₂, at a total pressure of 1×10^{-2} Torr. The sputtering plasmas were produced by an application of radio frequency signal, RF, 13.56 MHz, 100W, to the sample holder during grinding of the topmost electrode. The depositions were performed during 1500 s in an atmosphere of 70% hexamethyldisiloxane (HDMSO), 15% O₂, and 15% argon by the application of RF (13.56 MHz, 100 W) to the substrate holder. The background pressure and the working gas pressure were maintained at 2.0×10^{-2} and 1.8×10^{-1} Torr, respectively. Then, a final plasma oxidation treatment was conducted for 300 s at an atmosphere of 100% O₂ at 2×10^{-2} Torr of background pressure and 9.5×10^{-2} Torr of working pressure. This entire process was performed twice per disc, resulting in multilayered films.

C. Electrochemical test

The tests were conducted in an electrochemical cell made of polysulfone. A potentiostat (Interface 1000, Gamry Inc.) was used for the corrosion measurements. All measurements were performed by a standardized method of three-electrode cells in accordance with the instructions of the American Society for Testing and Materials (ASTM) (G61-86 and G31-72). A saturated calomel electrode (SCE) was used as a reference electrode (RE), a graphite rod as the counterelectrode (CE), and the exposed surface of a cpTi disc as the working electrode (WE). The exposed area of cpTi was determined by AFM for all groups (machined = 2.04 cm², sandblasted = 2.59 cm², PEO = 2.08 cm², GDP = 1.82 cm²). Artificial saliva at different pHs (3.0, 6.5, and 9.0) and SBF (pH 7.4) were used as electrolyte solutions to mimic the oral environment and the blood plasma, respectively. The composition of artificial saliva (g/L) was KCl (0.4), NaCl (0.4), CaCl₂ · 2H₂O (0.906), NaH₂PO₄ · 2H₂O (0.690), Na₂S · 9H₂O (0.005), and urea (1).⁷ Different pH values were obtained by the addition of lactic

acid (acid pH) or NaOH (basic pH) in an appropriate amount. The composition of the SBF (g/L) was NaCl (12.0045), NaHCO_3 (0.5025), KCl (0.3360), K_2HPO_4 (0.2610), Na_2SO_4 (0.1065), 1M HCl (60 mL), $\text{CaCl}_2 \cdot 2\text{H}_2\text{O}$ (0.5520), and $\text{MgCl}_2 \cdot \text{H}_2\text{O}$ (0.4575).³⁸ Tris was used to achieve a pH = 7.4. During the test, the electrolyte temperature was maintained at $37 \pm 1^\circ\text{C}$.

To standardize the oxide layer of the cpTi surfaces, a cathodic potential (-0.9 V vs. SCE) was applied for 10 min. The open circuit potential (OCP) was monitored for a period of 3600 s for evaluation of the free corrosion potential of the material in each electrolyte solution. After stable OCP values were reached, electrochemical impedance spectroscopy (EIS) was conducted at a frequency of 100 KHz to 5 mHz, with the AC curve in the range of ± 10 mV applied to the electrode as a corrosion potential so that we could observe the permeability of the electrolyte through the coating and evaluate the oxide passive layer.^{7, 33, 36, 39, 40} EIS data were used to determine the real (Z') and imaginary (Z'') components of the impedance as plotted in Nyquist, Bode ($|Z|$) and phase angle. The EIS results were analyzed by means of Echem Analyst software (provided by Gamry Instruments) and fitted to an appropriate equivalent electrical circuit to quantify the corrosion kinetics and oxide film formations. Then, the specimens were polarized from -0.8 V to 1.8 V at a scan rate of 2 mV/s.³⁶ The corrosion data were obtained from potentiodynamic polarization curves. The Tafel extrapolation method (Echem Analyst Software, Gamry Instruments) was used to obtain the corrosion potential (E_{corr}), corrosion current density (i_{corr}), and Tafel cathodic (b_c) and anodic (b_a) slopes. The passivation current density (i_{pass}) corresponds to the current value in the transition between the active and the passive regions expressed in the polarization curve. All tests were repeated at least five times to ensure reliability and reproducibility.

D. Surface characterization

1. Scanning electron microscopy (SEM) and energy-dispersive spectroscopy (EDS) analyses

SEM was used to characterize the film morphologies and EDS was conducted to evaluate the chemical composition of treated surfaces. Elementary chemical analysis in small volumes (around 1 μm^3) was performed. The thicknesses of PEO and GDP films were also determined. For the PEO group, the disc was cut in half by means of a precision cutting system (Exakt Advanced Technologies) and embedded in polyester resin (Teclago). The cross-sectional area was then ground in SiC abrasive papers (from #320 to #1200) (Teclago) and mirror-finished with a polishing cloth (Teclago) and alumina suspension (Teclago). The cross-sectional area was viewed under SEM. For the GDP group, an adhesive taper (Kapton, 3M) covered half of a glass slide while film deposition and treatment cycles were conducted. The adhesive taper was then removed, and the step between the untreated and treated areas was measured by a profilometer (Dektak 150-d, Veeco) (2000- μm cutoff at a constant time of 15 s).

2. X-ray photoelectron spectroscopy (XPS) analysis

XPS analysis was also used to obtain the chemical composition of the oxide layers. The spectrometer (Vacuum Scientific Workshop, VSW HA100) with a hemispherical analyzer was operated in constant transmission mode, resulting in a line width of 1.6 eV for Au 4f_{7/2}. The electron radiation for excitation was Al K α , 1486.6 eV. Pressure less than 2×10^{-8} mbar was used during the measurements. Surface charging was corrected by fixing the C1s line at 284.6 eV.⁴¹

3. Atomic force microscopy (AFM)

The 3D surface topography of different cpTi surfaces was analyzed by AFM (5500 AFM/SPM, Agilent Technologies). Images of 50 \times 50 μm were obtained in non-contact mode, and two distinct

areas of the cpTi surface were chosen for analysis. Image processing was performed with specific software (Gwyddion v 2.37; GNU General Public License).³⁶

4. X-ray diffraction (XRD) analysis

The crystalline composition of the oxides formed on the modified surfaces was analyzed by means of an x-ray diffractometer (XRD; Panalytical, X'Pert³ Power). CuK α radiation ($\lambda = 0.15418$ nm) operating at 40 kV and 50 mA for a scan range of 2θ from 20° to 70° was used.⁴²

5. Profilometry (surface roughness)

The surface roughness (Ra - arithmetic mean) was measured by means of a profilometer (Dektak 150-d, Veeco) with a 500- μ m cutoff, at a constant time of 12 s. Three measurements were obtained for each cpTi disc and then averaged.⁴³

6. Vickers microhardness

The Vickers microhardness of cpTi surfaces was calculated by means of a microhardness tester (Shimadzu HMV-2000 Micro Hardness Tester, Shimadzu Corporation) at room temperature (22 ± 2 °C). A 0.5 Kgf load was applied for 15 s, and the hardness was expressed in Vickers hardness units (VHN). The microhardness values were calculated according to the formula $VHN\ 2P = \sin(136^\circ/2)/d^2$, where P = load applied and d = distance between the diagonals of the indentation.⁴⁴ The test was repeated four times and at four points randomly distributed on the surface of each disc. The average of four replications corresponds to the value of VHN.

7. Surface energy

The analysis of the surface energy was measured according to the protocol suggested by Combe *et al.*⁴⁵ with the assistance of a goniometer (ramé-hart Instrument Co.). For the

determination of surface energy, the measurement of the contact angle between the disc surface and a sessile drop of diiodomethane (dispersive component) and deionized water (polar component) was conducted. This measurement was performed in three drops of each liquid at room temperature ($21 \pm 1^\circ\text{C}$) and controlled humidity. Each sessile drop ($0.2 \mu\text{L}$) was deposited onto the disc surface through an automatic dispenser coupled to the goniometer. The image obtained was immediately captured by the device, and the contact angle formed by the liquid on the substrate surface was automatically measured by the ramé-hart DROPimage Standard software (ramé-hart Instrument co.). The polar and dispersive components and the surface free energy were obtained.⁴⁵

E. Protein adsorption

For an understanding of how the proteins present in blood serum interact with different surface treatments, adsorption of albumin, fibrinogen, or fibronectin (Sigma–Aldrich) was investigated separately. The discs were sterilized by gamma radiation ($0.87 \pm 0.05 \text{ kGy}$) prior to being tested. The discs were incubated in 24-well culture plates containing $100 \mu\text{g/mL}$ of albumin, fibrinogen, or fibronectin in phosphate-buffered saline (PBS) (Gibco, Life Technologies) under horizontal stirring (75 rpm) at 37°C . After 2 h of incubation, the protein solution was aspirated and the discs were washed three times in PBS for the removal of non-adherent proteins.⁴⁶ The protein adsorption was measured by the bicinchoninic acid method (BCA Kit, Sigma–Aldrich) with bovine serum albumin as standard. The discs were transferred to cryogenic tubes containing 1 mL of PBS and were sonicated in a Cup Horn (5.5" cup, Q500, Qsonica) at an amplitude of 80% for 60 s. The discs were then vortexed for 60 s to remove the absorbed protein from the cpTi surface. The BCA kit quantifies only proteins in solution. In a microtiter plate of 96 wells, a $150\text{-}\mu\text{L}$ quantity of the sonicated suspension was added to $150 \mu\text{L}$ of a mixture with reagents A and B. The microplate was incubated at 60°C for 1 h, after which the absorbance of the solution was measured in a microplate spectrophotometer reader (Multiskan, Thermo Scientific) at a wavelength of 562 nm, according to

the manufacturer's recommendation. Protein concentration was calculated based on a standard curve prepared with bovine serum albumin (0.5 to 30 µg/mL of protein).

F. Statistical analyses

Statistical analyses were performed with statistical software (SPSS v.20.0, SPSS Inc.). Two-way ANOVA was used to evaluate the effects of surface treatment (factor 1) and electrolyte type (factor 2) on the electrochemical (R_p , CPE, E_{corr} , I_{corr} , and I_{pass}), roughness, microhardness, and surface energy data. The influence of surface treatment on the adsorption of blood serum proteins was tested by one-way ANOVA. The Bonferroni test was used as a post hoc technique for multiple comparisons ($\alpha = 0.05$). In this study, with five specimens per group, the observed power to detect a medium size effect (0.5, according to Cohen effect size statistics) for this study was > 0.8 .

III. RESULTS AND DISCUSSION

1. Electrochemical stability of cpTi with different surface treatments

1.1. Open circuit potential (OCP)

Figure 2 shows the OCP evolution as a function of time for all groups in the different electrolyte solutions. The PEO group showed the most positive values of OCP (values ranging from -75 to 250 mV vs. SCE) when compared with those of other groups: control (values ranging from -350 to -175 mV vs. SCE), sandblasted (values ranging from -250 to 50 mV vs. SCE), and GDP (values ranging from -400 to -200 mV vs. SCE). These results may indicate improvement of the corrosion tendency of the PEO group (tending to noble electrochemical potential), since more positive OCP values show a better corrosion behavior. The positive potential values observed in the PEO group may be attributed to the presence of a thick coating and the formation of a stable oxide film³⁶ that may protect the Ti surface.

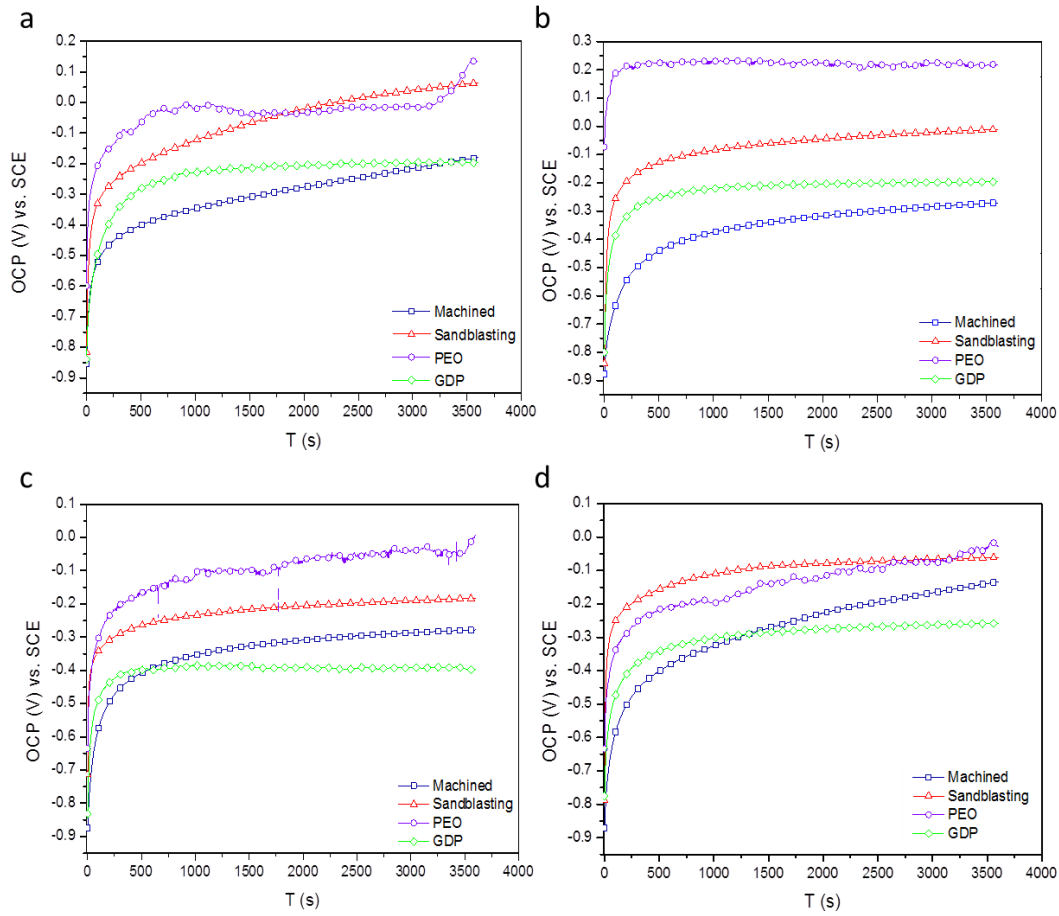


FIG. 2. Open circuit potential (OCP) diagrams for all groups immersed in solutions of artificial saliva (a) pH 3.0, (b) pH 6.5, (c) pH 9.0, and (d) SBF at 37°C for 1 h.

1.2. Electrochemical impedance spectroscopy (EIS)

A Nyquist plot (real component - Z_{real} of impedance vs. imaginary component - Z_{img} of impedance) is represented in Fig. 3. An increase in the diameter of the semicircular loop indicates an improvement in film stability, and a decrease in the semicircular diameter loop indicates a reduction in passive film resistance.⁴⁷ The machined and sandblasted groups showed a reduction in the semicircular diameter of the capacitance loop, regardless of the electrolyte type, which suggests a negative influence of these surface treatments on the electrochemical behavior of cpTi. The GDP group showed intermediate values. For the PEO group, a higher amplitude of the semicircular diameter of the capacitance loop was noted, which indicates improved corrosion resistance. A large

difference in magnitude was found between the controls and the experimental groups. Based on that, the Nyquist plots were magnified for better visualization.

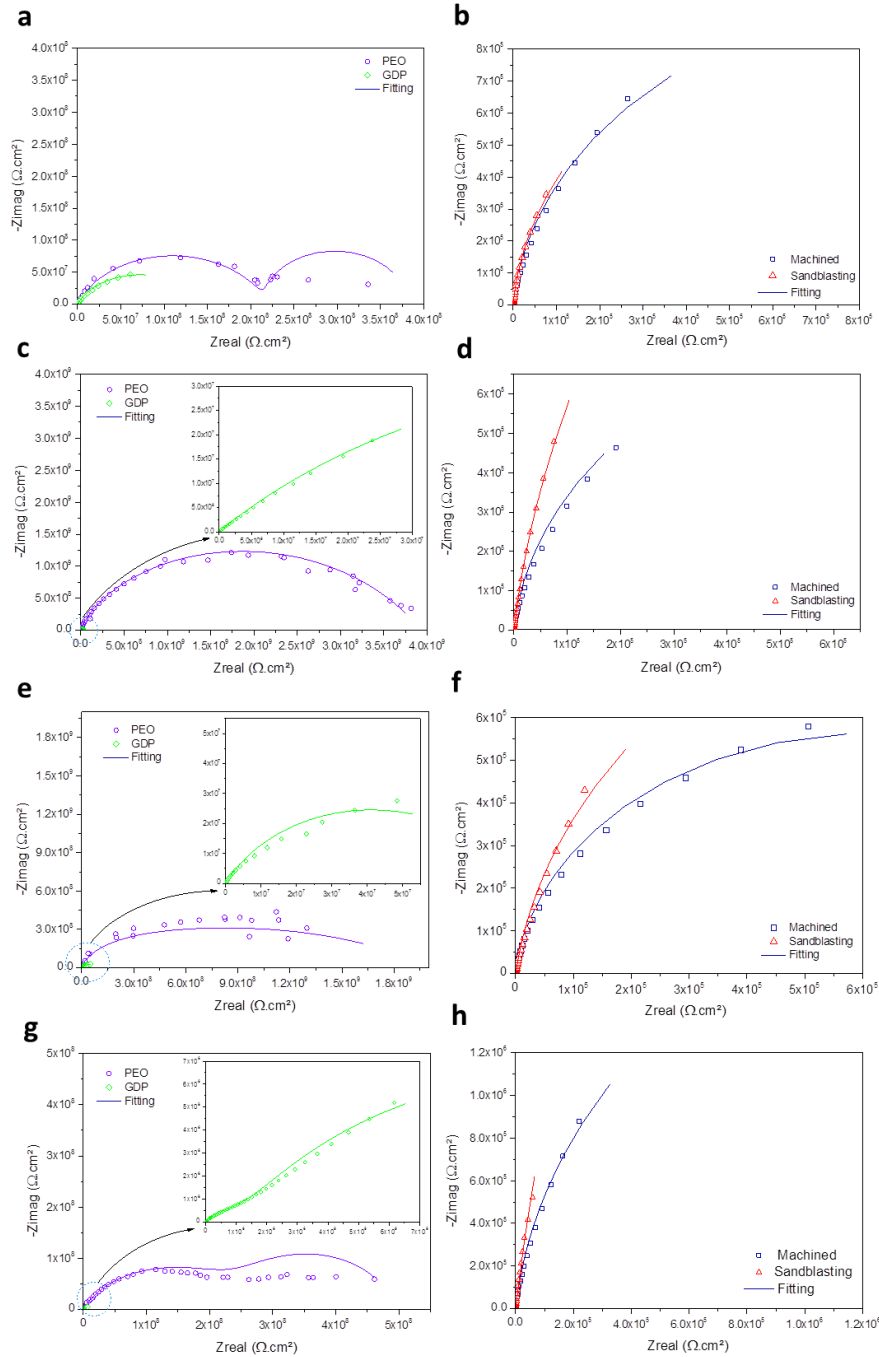


FIG. 3. Nyquist diagrams of EIS responses of control, sandblasted, PEO, and GDP groups immersed in artificial saliva (a-b) pH 3.0, (c-d) pH 6.5, (e-f) pH 9.0, and (g-h) SBF. Symbols represent experimental data and solid lines fitted data. Magnified graphs were plotted for better visualization.

The EIS results represented by the Bode plot (Fig. 4) showed that the PEO-treated surfaces exhibited the highest total impedance values (as can be seen in the y axis of each graph) in all different electrolytes. This behavior indicates an improvement of the electrochemical properties of the cpTi, since high impedance values at low frequencies suggest the formation of a highly stable oxide film on the substrate surface, which may lead to improved electrochemical stability. The presence of Ca and P in the PEO surface acts as a ceramic barrier that reduces the diffusion of ions from and to the cpTi surface.³⁶ Contrasting behavior was observed in machined and sandblasted groups, which exhibited very low impedance values. Similar results were obtained by Barranco *et al.*,⁴⁸ wherein machined and sandblasted Ti6Al4V alloy surfaces exhibited low impedance values. Regarding electrolyte solutions, in general, artificial saliva with pH 6.5 and 9.0 showed the highest total impedance values.

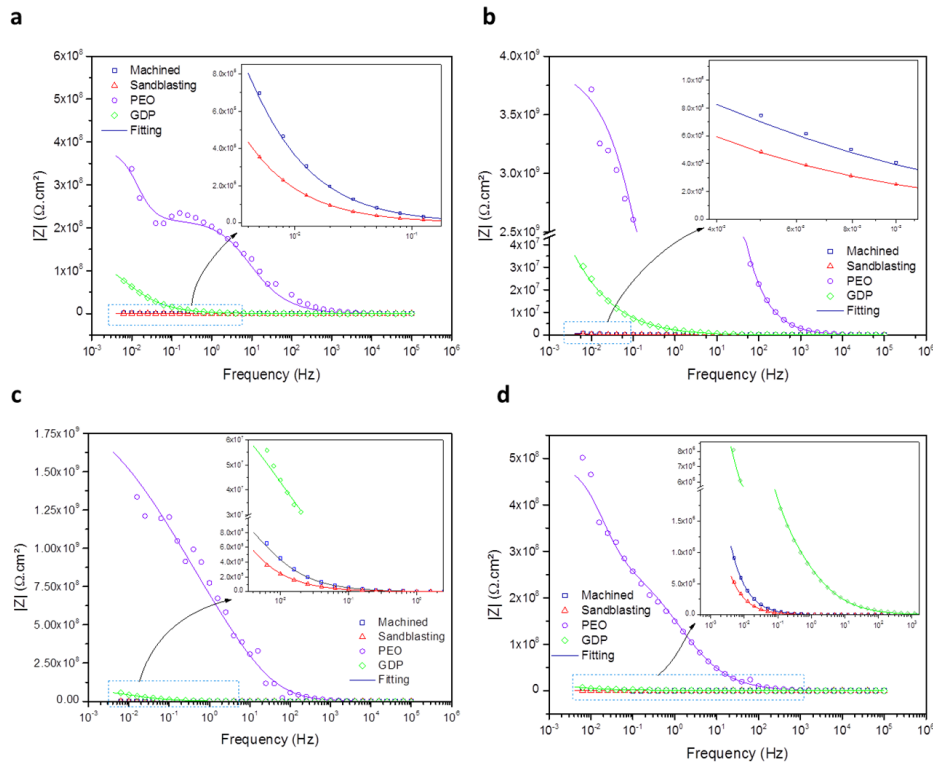


FIG. 4. Impedance modulus of all surface treatments of cpTi immersed in artificial saliva (a) pH 3.0, (b) pH 6.5, (c) pH 9.0, and (d) SBF. Symbols represent experimental data and solid lines fitted data. Magnified graphs were plotted for better visualization.

Figure 5 shows the graphs of phase angles, wherein machined and sandblasted surfaces showed only one time constant, which indicates the formation of a compact oxide layer. Two time constants can be observed for the PEO group, which reveals the formation of an inner compact layer and an outer porous layer. The first time constant at high frequency indicates the dielectric property of the porous coating of PEO, and the second time constant at medium frequencies is the barrier layer.⁴⁹ In the GDP group, three time constants can be noted, indicating a structure composed of a homogeneous and compact inner layer and two outer porous layers.⁵⁰ Moreover, it is interesting to note that, at high frequencies, phase angles of the PEO and GDP groups showed high values (around 80-90°), indicating an improvement of the electrochemical stability of cpTi when subjected to these treatments.

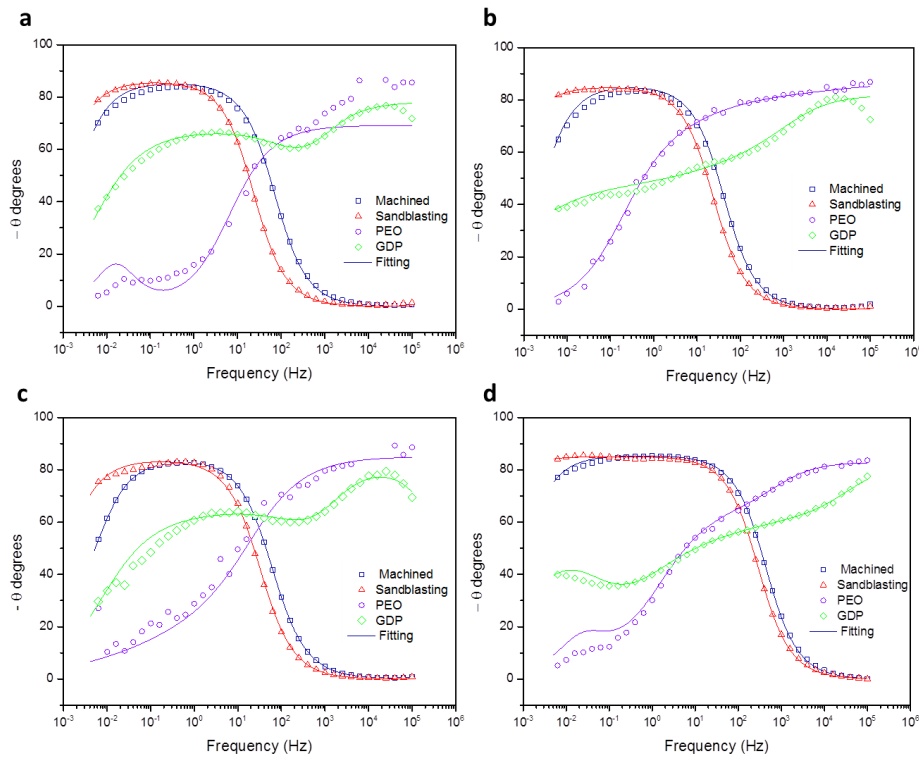


FIG. 5. Phase angles of all surface treatments of cpTi immersed in artificial saliva (a) pH 3.0, (b) pH 6.5, (c) pH 9.0, and (d) SBF. Symbols represent experimental data and solid lines fitted data.

Figure 6 shows the equivalent circuits used for simulation of the electrical parameters of the surface. The values of chi-square (χ^2) were in the order of 10^{-3} - 10^{-4} , indicating that the fitted data are

in agreement with the experimental data. For an understanding of the data impedance of machined and sandblasted surfaces, a simple electrical circuit was adopted, consisting of R_{sol} (solution resistance), R_1 (polarization resistance), and CPE (constant phase element). For good fit and a minimized surface heterogeneity factor, capacitance was replaced by the CPE.⁵¹ For PEO-treated samples immersed in artificial saliva (pHs 3.0, 6.5, and 9.0), an equivalent circuit consisting of two pairs of elements was used, in which R_1 represents the resistance of the pores, CPE1 the capacitance of the oxide layer, and R_2 and CPE2 represent resistance to electrical charge transfer and the capacitance of the double layer of the substrate, respectively.⁵² For the GDP-treated surface and the PEO surface immersed in SBF, the electrical circuit used was composed of R_{sol} , R_1 , and CPE1, representing the resistance and capacitance of the oxide film formed on the surface, respectively. R_2 and CPE2 describe the electrochemical reactions occurring in the passive layer-metal interface, while R_3 and CPE3 describe the ion diffusion phenomena in the oxide layer. The use of this circuit is considered valid for the study of Ti under passive conditions.⁵⁰

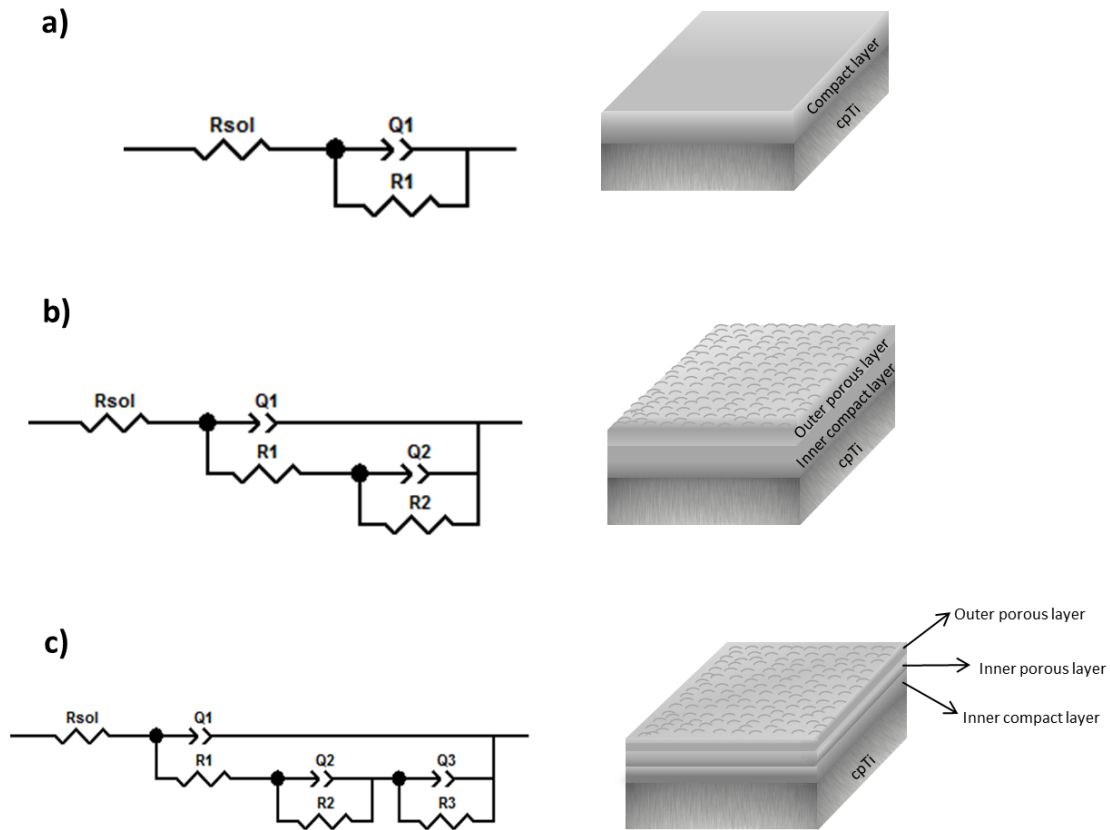


FIG. 6. Equivalent circuits used to fit EIS data. Circuits used in the (a) machined and sandblasted groups, (b) PEO group, and (c) PEO group (immersed in SBF) and GDP group.

The polarization resistance (R_p) and capacitance (CPE, represented as Q) data are shown in Table I. Total capacitance (Q_{tot}) represents the capacity for ionic changes in the electrolytic medium and is inversely proportional to total polarization resistance (R_{tot}), which measures the capacity to resist those ionic changes.⁷ For most electrolyte conditions, machined and sandblasted groups showed the lowest values of R_{tot} and higher values for Q_{tot} ($p < 0.05$). These findings are in agreement with the results obtained by Burnat *et al.*,⁵³ wherein a Ti6Al4V alloy subjected to sandblasting showed lower corrosion stability than did the machined surface. According to Barranco *et al.*,²⁷ the stability of the film formed on the sandblasted surface with aluminum oxide particles was severely affected by the impact of particles against the substrate. The stress accumulated at various points of

the deformed surface, generated by the impact of the particles, resulted in breakdown of the oxide film formed on the surface, increasing susceptibility to corrosion and promoting the release of metallic ions. Moreover, Barranco *et al.*⁴⁸ showed that the increase in capacitance of Ti subjected to sandblasting was due to an increased surface area available in the ratio of the greatest surface roughness presented by this group. In contrast, higher values of R_{tot} were noted for the PEO and GDP groups when compared with the other groups, wherein PEO, in artificial saliva at pH 6.5, presented the highest values ($p < 0.05$). The mechanism of corrosion protection of the PEO coating is determined by the diffusion of reacting species through the coating and resistance of the inner dense area of the coating next to the substrate.⁵⁴ According to Vargas *et al.*,³¹ it can be hypothesized that GDP, by modifying the oxide layer in two stages — first removing contaminants rich in hydrocarbons and other elements and then promote a "smoothing" of the substrate surface, resulting in a cleaner and more uniform oxide layer — promotes the formation of a more stable passive film. Therefore, following a similar pattern, the lowest values for Q_{tot} were found for the PEO group, followed by the GDP group ($p < 0.05$).

Regarding the electrolytic solutions, acidic artificial saliva showed higher Q_{tot} values for the machined and sandblasted groups ($p < 0.05$). This observation is in agreement with those of previous studies demonstrating that solutions with acid pH may cause dissolution of the oxide layer.⁵⁴ According to Barao *et al.*,⁷ acidic saliva accelerates the ion exchange between Ti and saliva, *i.e.*, increases the capacitance values and reduces the corrosion resistance, which is in agreement with the present results. In contrast, the PEO and GDP groups were able to withstand the negative effect of the electrolyte ($p > 0.05$). Acidification of the saliva can unclog the pores of the external layer on the PEO surface; however, it may be speculated that denser coatings delay the penetration of ions into the substrate.⁵⁴ The values of R_{tot} and Q_{tot} represent the properties of the cpTi oxide layer.⁷

The n values show whether the CPE acted as an inductor, resistor, or capacitor. When $n = -1$, the CPE acted as an inductor, $n = 0$ as pure resistor, and $n = 1$ as an ideal capacitor. Based on our data, it is possible to assume that CPE acts as a non-ideal capacitor due to the variable relaxation

times induced by microscopic inhomogeneity at the electrode/electrolyte interface. For the PEO and GDP groups, the outer oxide layers exhibited lower n values, indicating the formation of a porous structure, which correlates with the proposed electrochemical circuits shown in Fig. 6.

1.3. Potentiodynamic polarization curves

It is clear that the PEO and GDP groups shifted the current density to lower values. The electrode potential was shifted to positive values when compared with those of controls. The PEO group presented the behavior of a ceramic- or polymer-like (electrochemically inert) surface, showing smooth and symmetric cathodic and anodic zones. The shift of the curves to the upper left area of the graph indicates a more passive character of the PEO- and GDP-treated samples in comparison with control groups (Fig. 7). Sandblasted surfaces showed lower electrochemical stability of the dynamic nature of the corrosion process, owing to the presence of current fluctuation and zones of passivation and depassivation.

TABLE I. Means (and standard deviations) of electrical parameters obtained from the equivalent circuit models for all groups.

Groups		R1 (MΩ·cm ²)	R2 (MΩ·cm ²)	R3 (MΩ·cm ²)	R _{tot} (MΩ·cm ²)	Q1 (nΩ ⁻¹ s ⁿ .cm ²)	n1	Q2 (nΩ ⁻¹ s ⁿ .cm ²)	n2	Q3 (nΩ ⁻¹ s ⁿ .cm ²)	n3	Q _{tot} (nΩ ⁻¹ s ⁿ .cm ²)	χ ² × 10 ⁻³
Machined	AS pH 3.0	2.57 (0.43)	-	-	2.57 (0.43) ^{aA}	37163.33 (3425.76)	0.94 (0.01)	-	-	-	-	37163.33 (3425.76) ^{aA}	1.69 (1.14)
	AS pH 6.5	3.23 (0.85)	-	-	3.23 (0.85) ^{aA}	31186.66 (2965.17)	0.95 (0.00)	-	-	-	-	31186.66 (2965.17) ^{aB}	0.81 (0.15)
	AS pH 9.0	1.39 (0.53)	-	-	1.39 (0.53) ^{aA}	27780.00 (3095.72)	0.94 (0.01)	-	-	-	-	27780.00 (3095.72) ^{aB}	1.36 (0.40)
	SBF	5.26 (2.51)	-	-	5.26 (2.51) ^{aA}	29843.33 (946.27)	0.94 (0.01)	-	-	-	-	29843.33 (946.27) ^{aB}	0.67 (0.34)
Sandblasting	AS pH 3.0	1.65 (0.87)	-	-	1.65 (0.87) ^{aA}	76580.00 (6463.69)	0.94 (0.00)	-	-	-	-	76580.00 (6463.69) ^{aA}	0.10 (0.12)
	AS pH 6.5	8.23 (2.87)	-	-	8.23 (2.87) ^{aA}	57573.00 (8212.48)	0.94 (0.01)	-	-	-	-	57573.00 (8212.48) ^{aB}	0.25 (0.13)
	AS pH 9.0	3.17 (2.15)	-	-	3.17 (2.15) ^{aA}	51150.00 (1456.81)	0.93 (0.01)	-	-	-	-	51150.00 (1456.81) ^{bC}	0.59 (0.24)
	SBF	20.25 (7.45)	-	-	20.25 (7.45) ^{aA}	47193.31 (3961.39)	0.94 (0.01)	-	-	-	-	47193.30 (3961.39) ^{bC}	0.33 (0.21)
PEO	AS pH 3.0	16.05 (0.74)	821.05 (475.95)	-	837.10 (476.69) ^{bA}	0.14 (0.01)	0.92 (0.02)	0.48 (0.01)	0.59 (0.04)	-	-	0.63 (0.01) ^{cA}	2.14 (0.11)
	AS pH 6.5	4.81 (1.59)	2486.53 (1496.13)	-	2491.35 (1494.91) ^{bB}	0.09 (0.03)	0.94 (0.05)	0.25 (0.06)	0.61 (0.01)	-	-	0.34 (0.09) ^{cA}	6.13 (1.49)
	AS pH 9.0	9.57 (5.22)	809.93 (45.69)	-	819.51 (48.98) ^{bA}	0.21 (0.05)	0.85 (0.02)	0.53 (0.11)	0.66 (0.05)	-	-	0.74 (0.08) ^{cA}	5.17 (1.11)
	SBF	1.59 (0.19)	121.20 (20.75)	676.56 (192.31)	799.35 (177.47) ^{bA}	0.15 (0.06)	0.94 (0.01)	1.74 (0.18)	0.67 (0.03)	1.41 (0.88)	0.50 (0.04)	3.25 (1.12) ^{cA}	3.76 (1.18)
GDP	AS pH 3.0	0.08 (0.01)	202.53 (50.53)	9.31 (0.58)	211.92 (6.99) ^{cA}	6.45 (0.33)	0.92 (0.05)	108.00 (32.90)	0.67 (0.04)	146.21 (80.32)	0.64 (0.08)	260.66 (49.73) ^{dA}	0.41 (0.28)
	AS pH 6.5	0.02 (0.00)	51.49 (7.66)	38.12 (2.57)	89.63 (9.81) ^{cA}	5.90 (0.95)	0.64 (0.01)	233.53 (10.90)	0.49 (0.11)	290.21 (68.26)	0.48 (0.23)	529.64 (75.15) ^{dA}	1.20 (0.24)
	AS pH 9.0	0.05 (0.01)	70.90 (13.51)	196.23 (27.11)	267.18 (37.87) ^{cA}	17.93 (6.36)	0.90 (0.04)	92.70 (5.05)	0.43 (0.06)	224.10 (8.79)	0.46 (0.22)	334.73 (17.78) ^{dA}	2.01 (0.09)
	SBF	0.00 (0.00)	11.15 (1.73)	10.06 (1.37)	21.21 (2.94) ^{aB}	10.86 (1.92)	0.89 (0.01)	591.13 (202.50)	0.62 (0.05)	2369.33 (288.71)	0.68 (0.08)	2971.52 (268.41) ^{dB}	1.41 (0.06)

Different lowercase letters indicate significant differences among surfaces in the same electrolyte solution. Different uppercase letters indicate significant differences among different electrolytes in the same surface ($p < 0.05$).

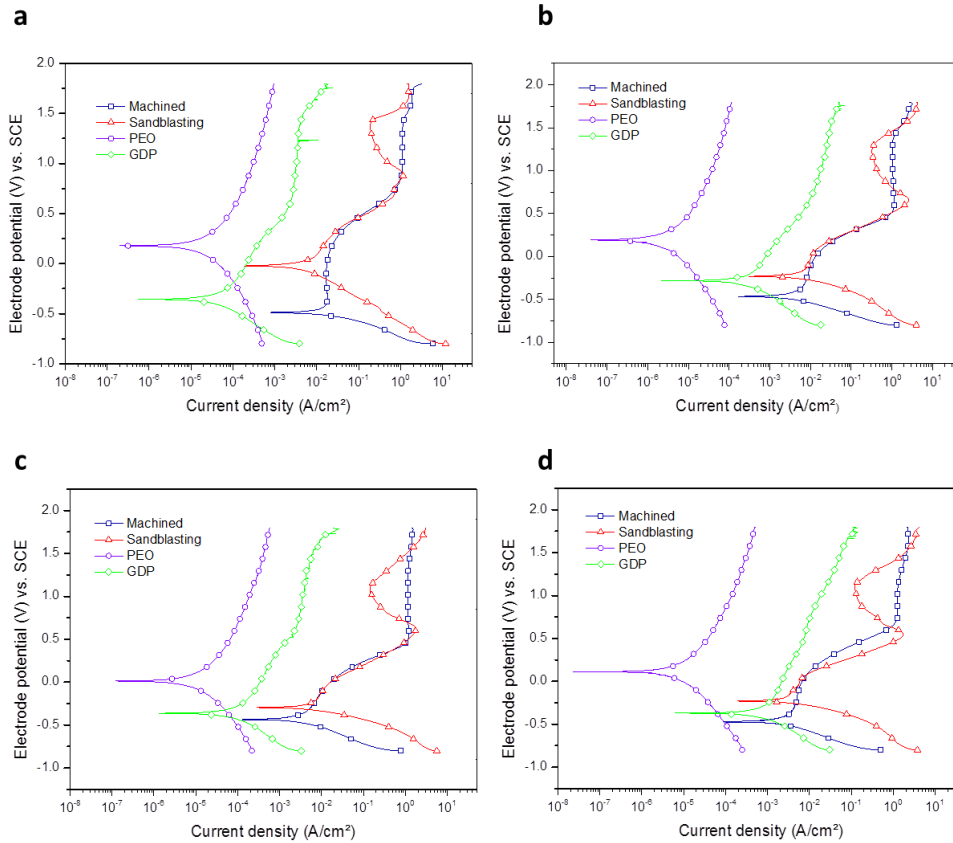


FIG. 7. Potentiodynamic polarization curves of all groups immersed in artificial saliva (a) pH 3.0, (b) pH 6.5, (c) pH 9.0, and (d) SBF.

The electrochemical parameters I_{corr} , E_{corr} , I_{pass} , and cathodic (b_c) and anodic (b_a) Tafel slopes can be seen in Table II. No Tafel linear region in the anodic slope (b_a) was noted for machined and sandblasted groups. Therefore, the parameters were obtained through Tafel extrapolation based on the cathodic slope (b_c). In general, groups treated with plasma (PEO and GDP) showed improved electrochemical behavior. Better performance in corrosion resistance was related to a more positive E_{corr} .⁵⁵ PEO also exhibited the highest values of E_{corr} and lower values of I_{pass} ($p < 0.05$), indicating nobler behavior as compared with that of other surfaces. Low I_{corr} values were noted for the PEO and GDP groups ($p < 0.05$). Furthermore, machined and sandblasted groups showed the largest I_{corr} values, suggesting unfavorable electrochemical properties. In addition, we noted that the sandblasted group did not have values for I_{pass} , since they could not be calculated due to current density fluctuations. Regarding the electrolyte solutions, artificial saliva at pH 3.0, in general, caused

the greatest I_{corr} values in all analyzed surfaces ($p < 0.05$). These results are in agreement with Q_{tot} and R_{tot} , where machined and sandblasted surfaces promoted the highest values for Q_{tot} and the lowest values for R_{tot} , and acidic artificial saliva showed higher capacitance values for the machined and sandblasted groups.

TABLE II. Mean (and standard deviation) values of electrochemical parameters obtained from the potentiodynamic polarization curves.

Groups		E_{corr} (V) vs. SCE	I_{corr} (nA cm ⁻²)	b_a (V dec ⁻¹)	$-b_c$ (V dec ⁻¹)	I_{pass} (nA cm ⁻²)
Machined	AS pH 3.0	- 0.44 (0.04) ^{aA}	77.97 (33.84) ^{aA}	-	0.13 (0.01)	12370 (272.21) ^{aA}
	AS pH 6.5	- 0.47 (0.03) ^{aA}	37.00 (4.08) ^{aB}	-	0.07 (0.09)	12726.67 (1161.44) ^{aA}
	AS pH 9.0	- 0.37 (0.06) ^{aA}	32.27 (7.09) ^{aBC}	-	0.18 (0.01)	12440 (304.47) ^{aA}
	SBF	- 0.40 (0.06) ^{aA}	18.60 (2.33) ^{aC}	-	0.19 (0.02)	12823.33 (155.35) ^{aA}
Sandblasted	AS pH 3.0	- 0.10 (0.07) ^{bA}	45.90 (5.46) ^{bA}	-	0.21 (0.03)	-
	AS pH 6.5	- 0.17 (0.05) ^{bA}	34.03 (12.96) ^{aA}	-	0.21 (0.02)	-
	AS pH 9.0	- 0.28 (0.04) ^{bB}	36.23 (12.44) ^{aA}	-	0.15 (0.01)	-
	SBF	- 0.21 (0.03) ^{bA}	28.87 (12.77) ^{aA}	-	0.18 (0.01)	-
PEO	AS pH 3.0	0.18 (0.01) ^{cA}	0.36 (0.25) ^{cA}	1.13 (0.07)	1.00 (0.04)	6.07 (3.42) ^{bA}
	AS pH 6.5	0.16 (0.01) ^{cA}	0.07 (0.03) ^{bA}	1.11 (0.10)	0.85 (0.04)	1.67 (1.18) ^{bA}
	AS pH 9.0	0.11 (0.51) ^{cAB}	0.16 (0.11) ^{bA}	1.17 (0.12)	0.88 (0.11)	3.46 (2.06) ^{bA}
	SBF	0.081 (0.04) ^{cB}	0.14 (0.08) ^{bA}	1.11 (0.11)	0.80 (0.09)	3.75 (2.15) ^{bA}
GDP	AS pH 3.0	- 0.34 (0.05) ^{aA}	0.71 (0.38) ^{cA}	0.60 (0.07)	0.28 (0.07)	144.21 (65.60) ^{cA}
	AS pH 6.5	- 0.31 (0.04) ^{aA}	0.13 (0.03) ^{bA}	0.64 (0.02)	0.34 (0.02)	540.57 (286.04) ^{cA}
	AS pH 9.0	- 0.34 (0.03) ^{aA}	0.16 (0.11) ^{bA}	0.82 (0.12)	0.39 (0.06)	324.97 (223.73) ^{cA}
	SBF	- 0.38 (0.02) ^{aA}	0.14 (0.08) ^{abB}	1.17 (0.01)	0.33 (0.01)	1836.00 (953.20) ^{cB}

Different lowercase letters indicate significant differences between and among surfaces in the same electrolyte solution. Different uppercase letters indicate significant differences between and among different electrolytes in the same surface ($p < 0.05$).

2. Surface characterization

Figure 8 shows the SEM micrographs and chemical compositions of the cpTi surfaces, determined by EDS. The presence of pores with wide openings (volcanic appearance) on the surfaces treated with PEO was noted. These findings are similar to the results obtained in previous studies.³⁶ According to Zhu *et al.*,⁵⁶ this event is associated with the effects of phosphorus and calcium on the development of the oxide film, due to the occurrence of sparks at the surface when the high voltage (over 265 V) is applied. In contrast, longitudinal grooves from the polishing process can be seen on the machined and GDP surfaces. Sandblasting with aluminum oxide promoted visible surface changes in cpTi, and crystals with standard sizes and shapes were noted. Regarding the chemical composition of the cpTi surfaces, we can see that the machined surface showed oxygen (O), carbon (C), and titanium (Ti) in its composition. Besides those elements mentioned above, peaks of aluminum (Al) were found on sandblasted surfaces due to the blasting process with 150 μm Al_2O_3 particles. The PEO group showed oxygen (O), titanium (Ti), carbon (C), calcium (Ca), and phosphorus (P) in its composition. The detection of calcium and phosphorus resulted from an electrolytic solution that was prepared by the dissolution of calcium acetate and of glycerophosphate disodium. The presence of Ca and P in the biofunctional film made the surface osteoconductive, stimulating bone growth and assisting in the rapid fixation of the implant.⁵⁷ The GDP group showed peaks of oxygen (O), carbon (C), and silicon (Si). The presence of silicon on the surface can be explained by the fact that hexamethyldisiloxane breaks down into methyl groups and silica during film deposition.⁵⁸ Active peroxide radicals are produced by O_2 and can incorporate functional groups, for example, C-O and C-OH, into the surface of the treated material.⁵⁹ These elements play an essential role in reducing the hydrophobicity of the surface,⁶⁰ which increases the chances of protein adsorption and hence cellular adhesion.

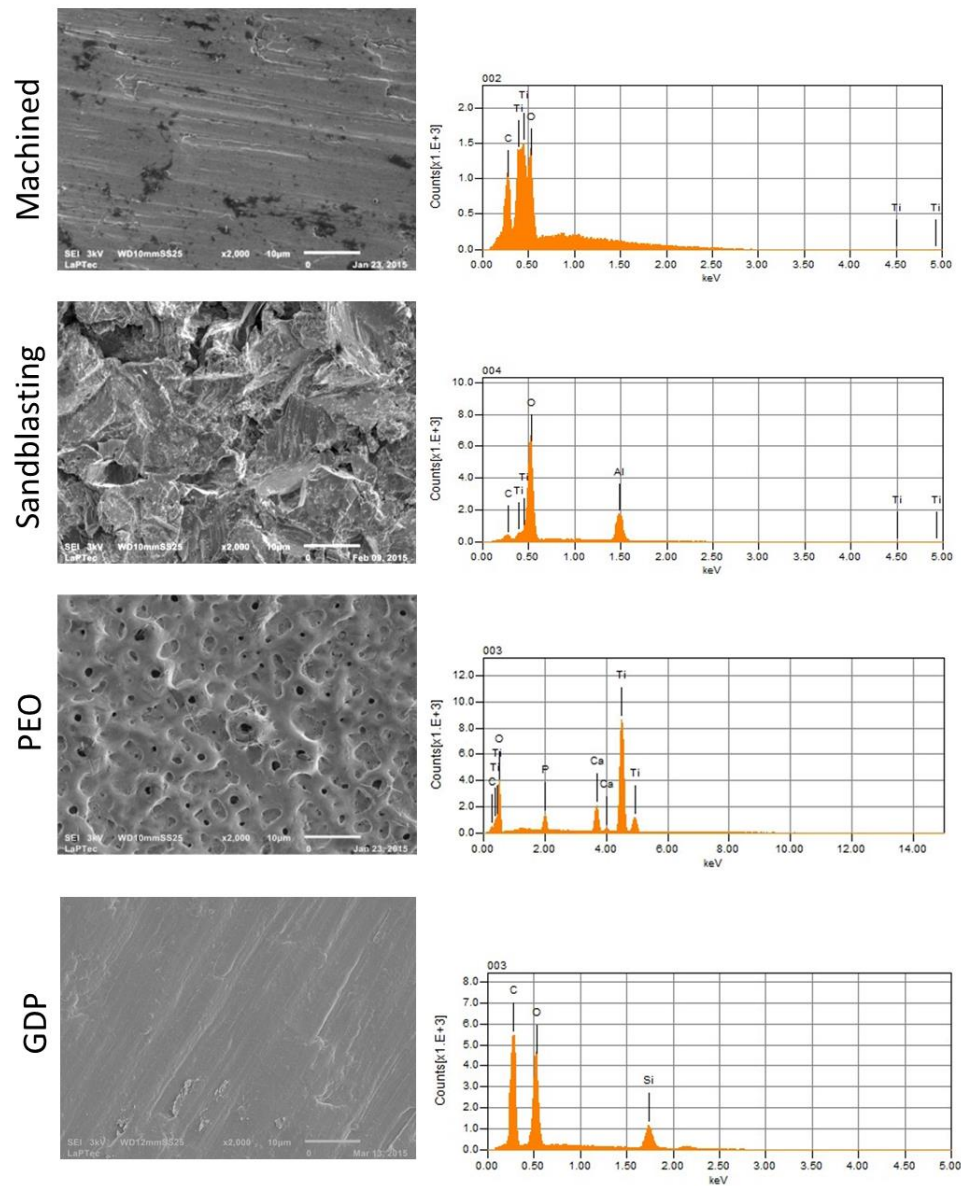


FIG. 8. SEM micrographs and EDS spectra with the chemical elements present in the oxide layer of different surface treatments.

The layer thicknesses produced by PEO and GDP can be seen in Fig. 9. In the PEO group, no cracks were observed on the film, and the layer thickness was approximately 5 μm, corroborating results from other studies.³⁶ Furthermore, we observed that there was no discontinuity between the film and the substrate, and, along the cross-section, there was no apparent defect, suggesting good adhesion of the formed film, which is probably another factor indicative of good corrosion

resistance.⁶¹ The graph allowed us to observe that the thickness of the oxide layer of the cpTi surface treated by GDP was 0.76 μm , which corroborates the findings of Hayakawa *et al.*⁵⁸

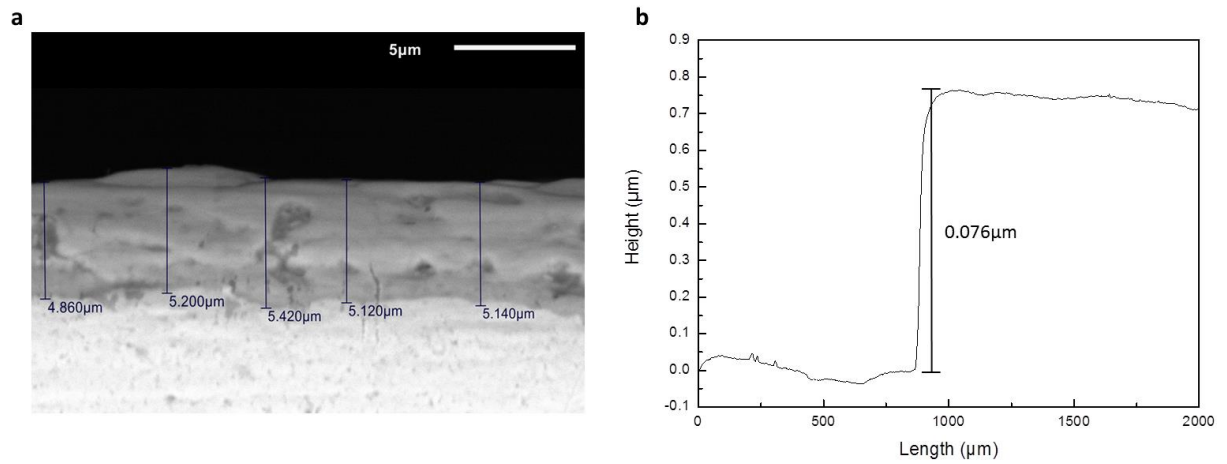


FIG. 9. Coating thickness. (a) Representative SEM micrograph of the oxide layer cross-section of the PEO group; (b) plot of film layer thickness of the group treated with GDP.

Figure 10 shows the XPS analysis, which revealed the chemical composition of the outer oxide layer formed on the surface of cpTi. The XPS results for machined surfaces showed the presence of peaks relating to Ti and O. Sandblasted surfaces showed all the elements mentioned above, plus an Al peak. On the surface subjected to PEO treatment, peaks at binding energies corresponding to O, Ca, and P were also observed. The GDP surface showed the presence of peaks related to O, Si, and C. Peaks over a range of 457.7 eV (Ti 2p_{3/2}) to 464.3 eV (Ti 2p_{1/2}) were found for the Ti 2p spectrum, similar to those for machined, sandblasted, and PEO groups, suggesting the connection of Ti and O, forming TiO₂. In O 1s spectra for the machined group, a peak at 529.5 eV was found to be related to O²⁻ ions, which possibly form the TiO₂ layer; in the sandblasted group, a peak centered at approximately 531.6 eV was found, which suggests that O²⁻ ions may be bonded to Al⁺³ ions to form Al₂O₃. Also, in relation to O 1s spectra, in the PEO group, the peak at 533.3 eV may be associated with P ions or CaP-based compounds, the 531.0 peak may be related to the sum of the contributions of TiO₂ and Ca compounds,⁶² and peaks at around 532.6 eV suggest the presence of

compounds formed by the Si-O bond to form SiO_2 on the surface treated with GDP.⁵⁸ For the band of Al 2p, a peak at 74.4 eV was observed for Ti subjected to sandblasting procedures, which indicates the formation of an Al_2O_3 compound.⁶¹ With respect to Ca 2p bands, it was possible to observe peaks at approximately 346.7 to 350.3 eV (Ca 2p_{3/2}) for the samples treated with PEO, which can be related to the formation of calcium phosphate compounds.⁶³ Regarding P 2p spectra, peaks at a range of 132.8 eV to 133.3 eV could be observed, which suggest the presence of calcium phosphate compounds $[\text{CaHPO}_4 \text{ and/or } \text{Ca}_{10}(\text{PO}_4)_6(\text{OH})_2(\text{HA})]$.⁶³ The Ca^{2+} and PO_4^{3-} ions react with OH^- ions under high temperature in microdischarge channels to produce HA on the TiO_2 matrix.⁶⁴ For the Si 2p band, a peak centered at approximately 102.8 eV was found in the GDP group, suggesting the presence of silicon oxide compounds formed by Si-O bonds.⁵⁸ Regarding C 1s spectra, it was possible to observe peaks at 288.6, 286.5, and 284.6 eV, which could be related to saturated hydrocarbons.⁶⁵

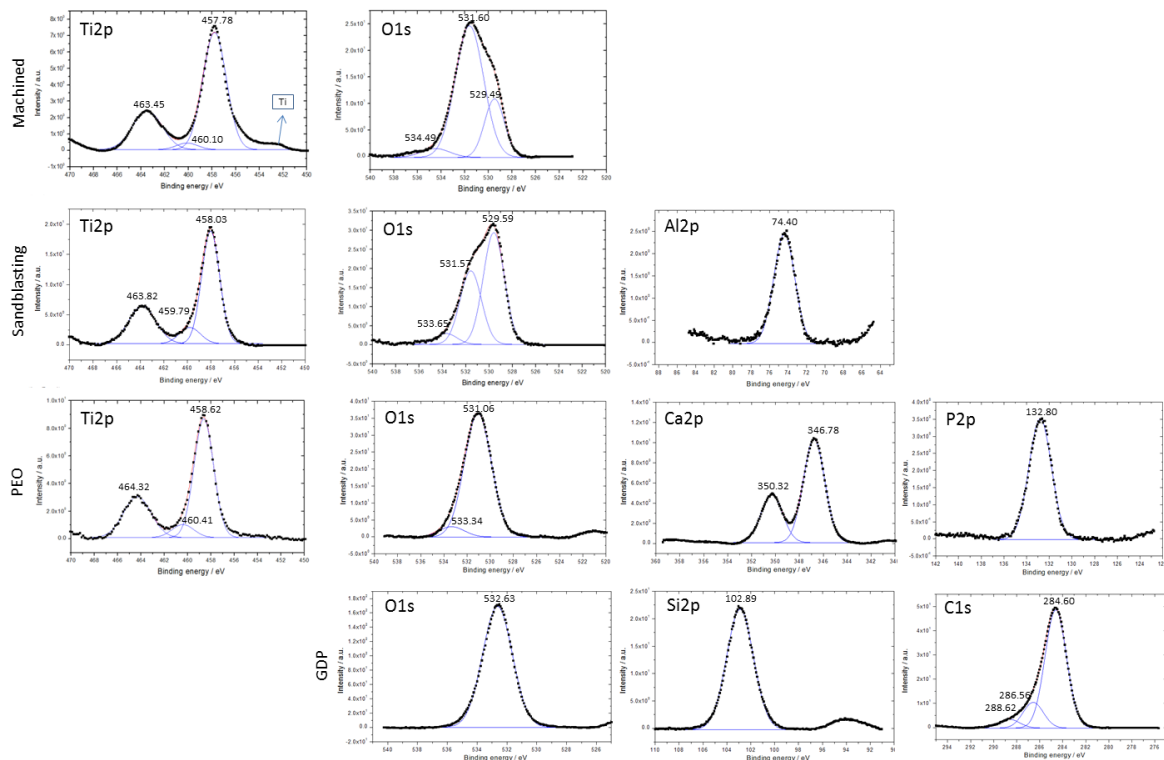


FIG. 10. XPS spectra of all surface treatments for Ti 2p, O 1s, Al 2p, Ca 2p, P 2p, Si 2p, and C 1s bands.

Atomic force microscopy (Fig. 11) was used to provide two- and three-dimensional information on the topography of cpTi as a function of surface treatment. The surfaces were free of cracks, packed thick, and composed of visible beads. Machined and GDP surfaces presented longitudinal grooves resulting from the polishing process. The sandblasting process promoted the formation of deeper valleys and salient peaks, whereas treatment with PEO promoted the formation of pores in the surface.

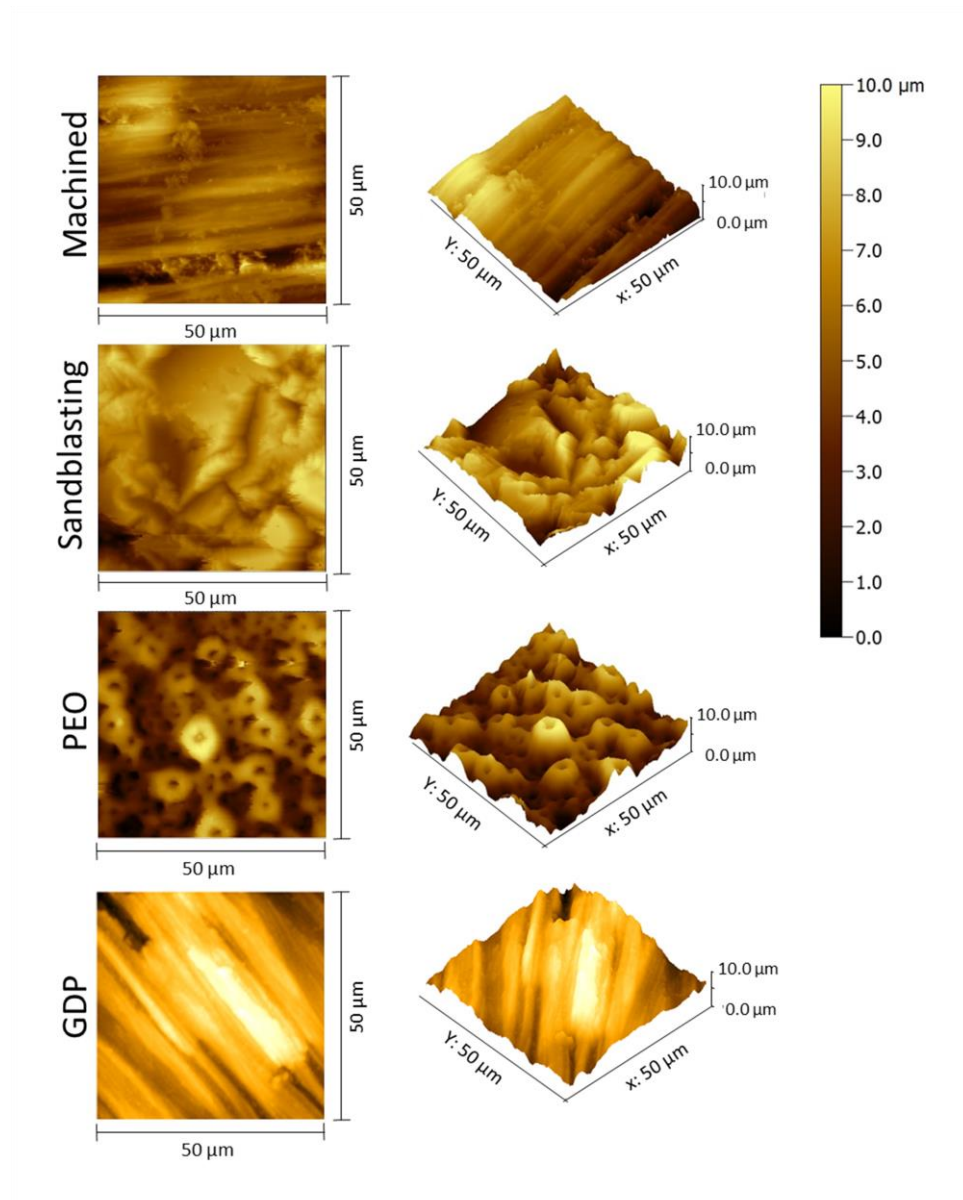


FIG. 11. AFM 2D and 3D images of the topographies of all surface treatments

The phase composition of oxides formed on the cpTi surface was analyzed by XRD. In Fig. 12, the analysis revealed that the PEO was the only group to show crystalline structures in the oxide layer, with the presence of rutile and anatase peaks, which have tetragonal crystal structure and are bioactive and biocompatible for bone implants in biomedical applications.⁶³ Anatase and rutile peaks adhere chemically to HA due to high bioactivity.⁶⁶ In addition, a semiquantitative analysis indicated that the PEO-treated surface was composed of 60% anatase, 33% rutile, and 7% of amorphous Ti. The other groups showed oxide layers with an amorphous structure. According to Durdu *et al.*,⁶⁷ early in the PEO treatment process, hydroxyl ions (OH^-) and Ti ions (Ti^{4+}) react with each other to form anatase (TiO_2) and rutile (TiO_2) phases in the microdischarge channels. Anatase begins to form in the first minutes and then transforms into rutile with increasing duration time. Anatase forms earlier than rutile because the temperature in the microdischarge channels at low-duration times is lower than that at high-duration times, explaining why larger percentages of anatase to rutile were found in the present study. The presence of rutile may also explain the better corrosion behavior of the PEO group.³⁶

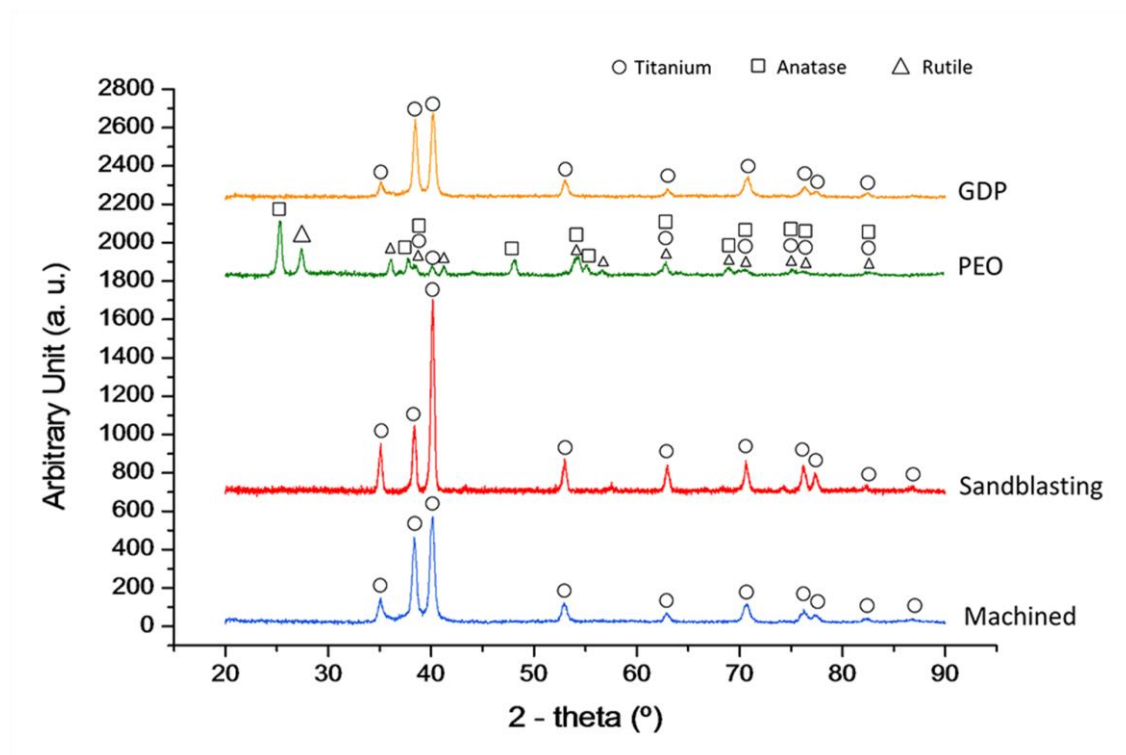


FIG. 12. XRD patterns obtained from all surface treatments.

Figure 13 shows the average Ra of cpTi subjected to different surface treatments before and after the electrochemical process. Surface treatments such as PEO and sandblasting increased the values of surface roughness of cpTi, and the highest Ra values were found for the sandblasted group ($p < 0.05$). It has been reported in the literature that surface roughness improves the osseointegration process when compared with smooth Ti.⁶⁸ The machined and GDP groups exhibited the lowest values of Ra and showed no statistically significant difference between them. The corrosion process, in general, did not affect the roughness characteristics of the material in any of the electrolyte solutions.

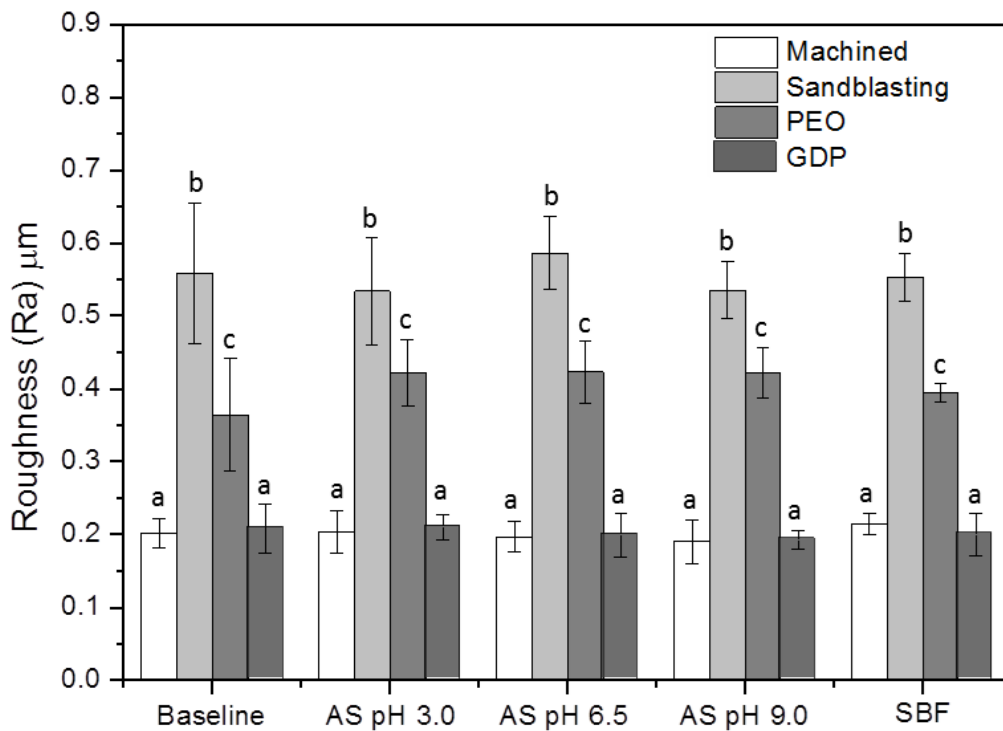


FIG. 13. Average roughness (Ra) and standard deviation for all surface treatments at baseline and after immersion in different artificial saliva solutions (pH 3.0, 6.5, and 9) and SBF. Different letters indicate significant differences within the electrolyte solution ($p < 0.05$).

The Vickers microhardness data are represented in Fig. 14. Treatment with PEO and sandblasting increased Vickers hardness values of cpTi when compared with the other groups ($p < 0.05$). Yang *et al.*⁶⁹ observed an increase in the hardness of Ti in treated vs untreated surfaces. The

increased surface hardness in the PEO group may be attributed to the presence of rutile.⁷⁰ Coatings containing aluminum oxide improved the hardness properties of cpTi.⁷¹ After the corrosion process, the Vickers hardness of all groups tended to reduce, and this trend was most pronounced in the PEO and sandblasted groups. However, even after the corrosion process, the hardness of the PEO and sandblasted groups tended to be higher than that observed in the machined and GDP groups. It can be speculated that the corrosion process degrades the most external oxide layer. For clinical applications, the increase of surface hardness by surface treatment could be recommended, because it increases the resistance of the material, contributing to the longevity of the implant.⁶⁹

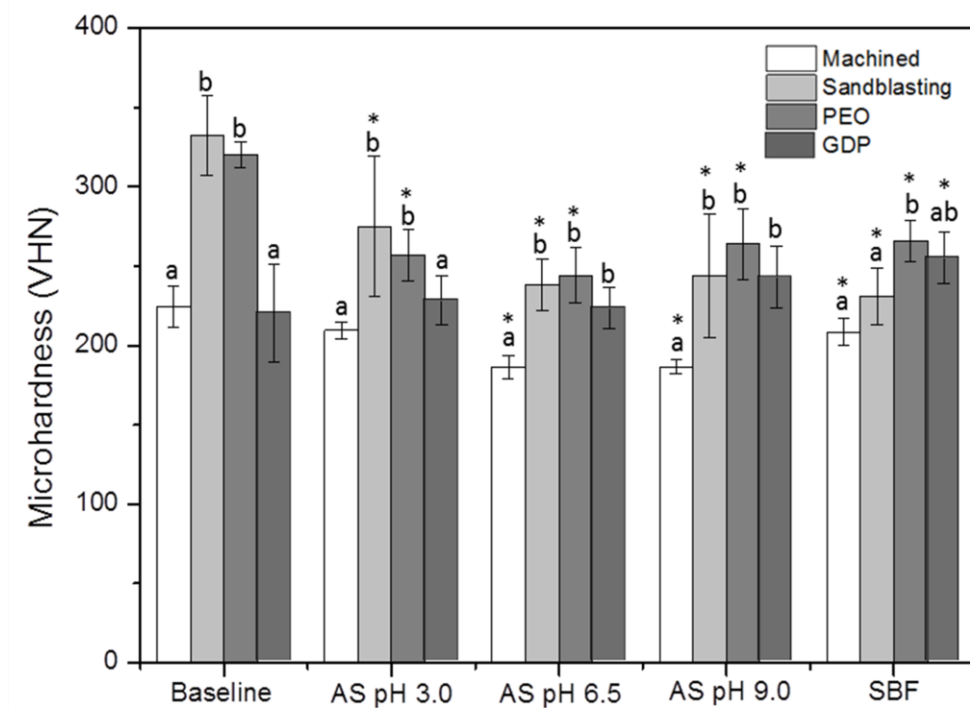


FIG. 14. Mean and standard deviation of Vickers microhardness (VHN) for all surface treatments at baseline and after immersion in different artificial saliva solutions (pH 3.0, 6.5, and 9) and SBF. Letters indicate significant differences among the surfaces in the same electrolyte solution ($p < 0.05$). * Significant differences between electrolyte solution and baseline within the surface type ($p < 0.05$).

Wettability and surface energy play an extremely important role in protein adsorption and, consequently, in osseointegration.⁷² Materials that have a higher surface energy show greater wettability and consequently are more hydrophilic and tend to adsorb proteins more easily.⁷³ When

the implant is inserted into the bone, a cascade of reactions occurs in the implant surface, and the first biological event is protein adsorption.⁷⁴ All these processes will be reflected in osseointegration, since the protein adsorption media interact between the substrate and the cell surface.⁷⁵ The wettability of the surface was analyzed by measurement of the contact angle. The surface energy data are shown in Fig. 15. The initial surface energy was higher in the group subjected to the GDP treatment ($p < 0.05$), suggesting higher hydrophilicity on the surface. The other groups had similar surface energy ($p > 0.05$). After the corrosion process, a significant reduction in the surface energy in the GDP group was noted in all electrolytes. In the machined, sandblasted, and PEO groups, the surface energy of cpTi tended to remain stable. It is possible that the corrosion process degraded the outer (hydrophilic) layer, exposing the organosilicone (hydrophobic) layer, which explains the reduction of surface energy for the GDP group after corrosion.

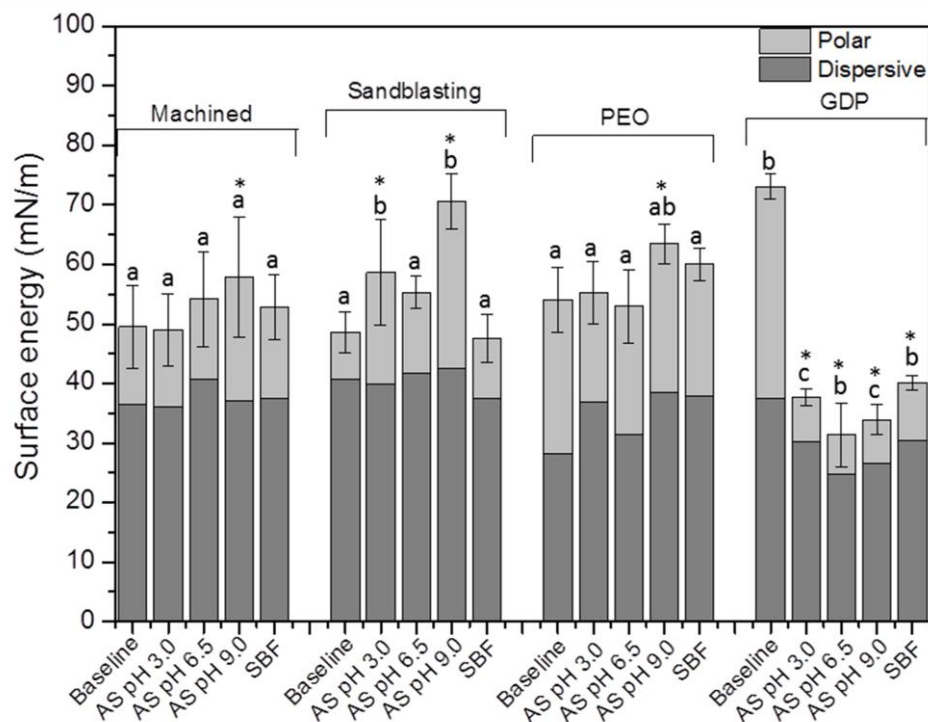


FIG. 15. Mean and standard deviation of surface energy (nM/m) for all surface treatments at baseline and after immersion in different artificial saliva solutions (pH 3.0, 6.5, and 9) and SBF. Letters indicate significant differences among the surfaces in the same electrolyte solution ($p < 0.05$). *Significant differences between electrolyte solution and baseline within the surface type ($p < 0.05$).

3. Blood serum protein adsorption

The results of adsorption of albumin, fibrinogen, and fibronectin as a function of the different surface treatments are represented in Fig. 16. For albumin, the PEO and sandblasted groups promoted greater protein adsorption ($p < 0.05$) and showed no statistically significant difference from each other ($p > 0.05$). For fibronectin adsorption, the PEO, sandblasted, and GDP groups showed greater protein adsorption ($p < 0.05$). According to Han *et al.*,⁷⁶ a conformational change in the fibronectin molecule may explain an increased adsorption in the GDP surface. Regarding the adsorption of fibrinogen, the PEO group presented the highest adsorption, followed by the sandblasted and GDP groups, which were similar. Yang *et al.*⁷⁷ showed that fibrinogen adsorption was higher on surfaces containing HA when compared with amorphous surfaces (TiO_2). The adsorption of fibrinogen is mediated by electrostatic interactions between the negatively charged TiO_2 and positively charged αC and is reversible.⁷⁸ Moreover, fibrinogen adsorption on HA is more effective because the positive Ca^{2+} ions and PO_4^{3-} ions available significantly increase the chances of fibrinogen interaction with the HA surface.⁷⁹ The binding of fibrinogen and HA can be caused by non-specific attractions between functional groups of the protein, positively charged, and hydroxyl groups of HA or through specific attractions between carboxyl groups of the protein, negatively charged, and Ca^{2+} ions present in the HA.⁷⁷ Therefore, these factors may explain the increased fibrinogen adsorption on surfaces treated with PEO, since CaP coatings provide more binding sites for fibrinogen than do sandblasted surfaces.

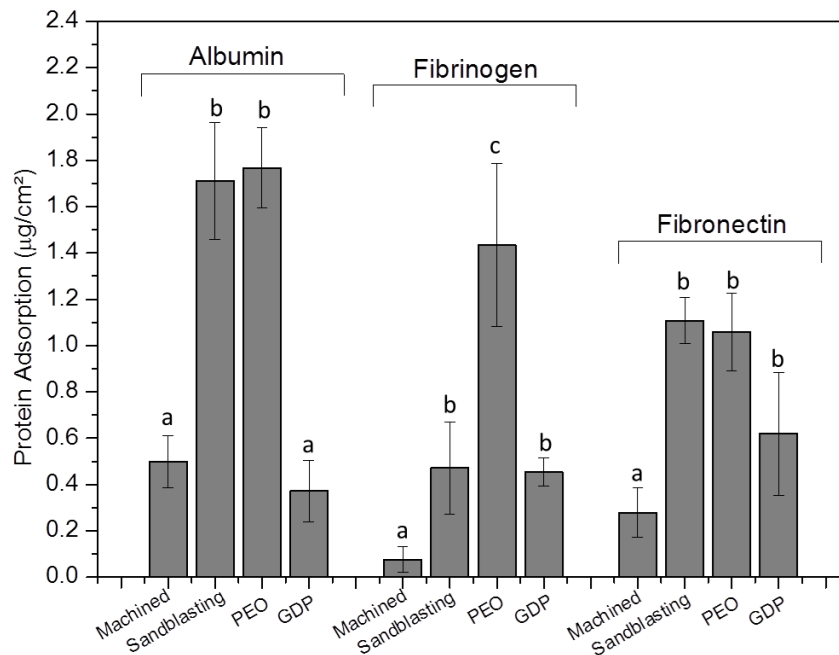


FIG. 16. Albumin, fibrinogen, and fibronectin adsorption as a function of different surface treatments of cpTi. Different letters indicate significant differences within the same protein ($p < 0.05$).

IV. CONCLUSIONS

In the present study, the successful synthesis of biofunctional Ti surfaces by plasma electrolytic oxidation and glow-discharge plasma has been demonstrated. Based on the results, plasma-treated samples were able to improve the electrochemical behavior of cpTi when compared with untreated and sandblasted surfaces. Regarding electrolyte solutions, acidic saliva reduced the corrosion resistance of cpTi. The presence of pores (volcanic appearance) on surfaces treated with PEO was noted through SEM and AFM. On PEO surfaces, no cracks were observed on the film, and the layer thickness was approximately 5 µm. A thin oxide layer of 0.76 µm was formed on cpTi surfaces treated with GDP. A crystalline structure in the oxide layer was found in the PEO group, with the presence of rutile and anatase peaks. The presence of Ca and P ions positively affected the adsorption of albumin, fibrinogen, and fibronectin, especially fibrinogen adsorption, by providing a greater number of binding sites for proteins. The sandblasted surfaces also showed great protein adsorption due to the high surface roughness. Therefore, future studies are suggested to assess the cell interaction with, and bone formation on, plasma surfaces. The synergistic interaction between

wear and corrosion (*i.e.*, tribocorrosion) is also warranted for an understanding of the degradation mechanisms of such coatings when used for implant applications. In addition, clinical trials are needed to evaluate the longevity of the implants with proposed surface treatments, specifically in dental and orthopedic applications.

ACKNOWLEDGMENTS

The authors thank the Fund for Teaching, Research and Extension Support (FAPEX) from the Univ. of Campinas (UNICAMP) (#653/13) for the master scholarship provided to the first author, the State of São Paulo Research Foundation (FAPESP) (#2013/08451-1), and the National Council of Technological and Scientific Development (CNPq) (#442786/2014-0 and #304908/2015) for grant support. The authors also express gratitude to Rita Vinhas from the Institute of Physics Gleb Wataghin (UNICAMP) for providing the facilities to conduct XPS analysis; Rafael Parra for his contributions and support in the Plasma Technology Lab at the Univ. Estadual Paulista (UNESP); and Elton José de Souza from the Department of Physics and Chemistry at UNESP for use of the AFM facility.

References

- ¹L. Schropp, A. Wenzel, and A. Stavropoulos, *Clin. Oral Implant Res.* **25**, 1359 (2014).
- ²F. Bassi, A. B. Carr, T. L. Chang, E. Estafanous, N. R. Garrett, R. P. Happonen, S. Koka, J. Laine, M. Osswald, H. Reintsema, J. Rieger, E. Roumanas, E. Estafanous, T. J. Salinas, C. M. Stanford, and J. Wolfaardt, *Int. J. Prosthodont.* **26**, 323 (2013).
- ³P. Gupta, G. Tenhundfeld, E. O. Daigle, and D. Ryabkov, *Surf. Coatings Technol.* **201**, 8746 (2007). ⁴A. C. Vieira, A. R. Ribeiro, L. A. Rocha, and J. P. Celis, *Wear* **261**, 994 (2006).
- ⁵J. C. M. Souza, M. Henriques, W. Teughels, P. Ponthiaux, J.-P. Celis, and L. A. Rocha, *J. Bio- Tribo- Corros.* **1**, 13 (2015).
- ⁶J. C. Souza, P. Ponthiaux, M. Henriques, R. Oliveira, W. Teughels, J. P. Celis, and L. A. Rocha, *J. Dent.* **41**, 528 (2013).
- ⁷V. A. Barao, M. T. Mathew, W. G. Assunção, J. C. Yuan, M. A. Wimmer, and C. Sukotjo, *Clin. Oral Implants Res.* **23**, 1055 (2012).
- ⁸L. Faverani, J. Fogaça, T. Machado, E. Silva, V. Barao, and W. Assunção, *J Bio- Tribo- Corros.* **1**, (2015).
- ⁹F. Nikolopoulou, *Implant Dent.* **15**, 372 (2006).
- ¹⁰D. G. Olmedo, M. L. Paparella, M. Spielberg, D. Brandizzi, M. B. Guglielmotti, and R. L. Cabrini, *J. Periodontol.* **83**, 973 (2012).
- ¹¹R. M. Urban, J. J. Jacobs, M. J. Tomlinson, J. Gavrilovic, J. Black, and M. Peoc'h, *J. Bone Joint Surg. Am.* **82**, 457 (2000).
- ¹²T. Hanawa, *J. Periodontal Implant Sci.* **41**, 263 (2011).
- ¹³Y.-C. Chang, S.-W. Feng, H.-M. Huang, N.-C. Teng, C.-T. Lin, H.-K. Lin, P.-D. Wang, and W.-J. Chang, *Clin. Implant Dent. Rel. Res.* **17**, 469 (2013).
- ¹⁴J. E. Davies, *J. Dent. Educ.* **67**, 932 (2003).
- ¹⁵Z. U. Rahman, W. Haider, L. Pompa, and K. M. Deen, *Mater. Sci. Eng. C* **58**, 160 (2016).
- ¹⁶Y. Li, S. Zou, D. Wang, G. Feng, C. Bao, and J. Hu, *Biomaterials* **31**, 3266 (2010).
- ¹⁷H. P. Felgueiras, L. Castanheira, S. Changotade, F. Poirier, S. Oughlis, M. Henriques, C. Chakar, N. Naaman, R. Younes, V. Migonney, J. P. Celis, P. Ponthiaux, L. A. Rocha, and D. Lutomski, *J. Biomed. Mater. Res. Part B: Appl. Biomater.* **103**, 661 (2014).
- ¹⁸A. R. Rafieerad, M. R. Ashra, R. Mahmoodian, and A. R. Bushroa, *Mater. Sci. Eng. C* **57**, 397 (2015).
- ¹⁹N. C. M. Oliveira, C. C. G. Moura, D. Zanetta-Barbosa, D. B. S. Mendonça, G. Mendonça, and P. Dechichi, *Mater. Sci. Eng. C Mater. Biol. Appl.* **33**, 1958 (2013).
- ²⁰K. N. Pandiyaraj, R. R. Deshmukh, R. Mahendiran, P. G. Su, E. Yassitepe, I. Shah, S. Perni, P. Prokopovich, and M. N. Nadagouda, *Mater. Sci. Eng. C Mater. Biol. Appl.* **36**, 309 (2014).
- ²¹K. Bazaka, M. V. Jacob, R. J. Crawford, and E. P. Ivanova, *Acta. Biomater.* **7**, 2015 (2011).
- ²²L. Hao and J. Lawrence, *J. Biomed. Mater. Res. A* **69**, 748 (2004).
- ²³T. Albrektsson and A. Wennerberg, *Int. J. Prosthodont.* **17**, 544 (2004).
- ²⁴P. G. Coelho, S. L. de Assis, I. Costa, and V. P. Thompson, *J. Mater. Sci. Mater. Med.* **20**, 215 (2009).
- ²⁵E. Eisenbarth, D. Velten, M. Muller, R. Thull, and J. Breme, *Biomaterials* **25**, 5705 (2004).
- ²⁶C. Aparicio, F. J. Gil, C. Fonseca, M. Barbosa, and J. A. Planell, *Biomaterials* **24**, 263 (2003).
- ²⁷V. Barranco, E. Onofre, M. L. Escudero, and M. C. Garcia-Alonso, *Surf. Coatings Technol.* **204**, 3783 (2010).
- ²⁸E. M. Szesz, B. L. Pereira, N. K. Kuromoto, C. E. B. Marino, G. B. de Souza, and P. Soares, *Thin Solid Films* **528**, 163 (2013).
- ²⁹X. Zhou and P. Mohanty, *Electrochim. Acta* **65**, 134 (2012).
- ³⁰C. T. Kwok, P. K. Wong, F. T. Cheng, and H. C. Man, *Appl. Surf. Sci.* **255**, 6736 (2009).
- ³¹E. Vargas, R. E. Baier, and A. E. Meyer, *Int. J. Oral Maxillofac. Implants* **7**, 338 (1992).
- ³²K. Bordji, J. Y. Jouzeau, D. Mainard, E. Payan, P. Netter, K. T. Rie, T. Stucky, and M. Hage-Ali, *Biomaterials* **17**, 929 (1996).
- ³³V. A. Barao, M. T. Mathew, W. G. Assunção, J. C. Yuan, M. A. Wimmer, and C. Sukotjo, *J. Dent. Res.* **90**, 613 (2011).

- ³⁴S. Li, J. Ni, X. Liu, X. Zhang, S. Yin, M. Rong, Z. Guo, and L. Zhou, *J. Biomed. Mater. Res. B Appl. Biomater.* **100**, 1587 (2012).
- ³⁵G. S. Shi, L. F. Ren, L. Z. Wang, H. S. Lin, S. B. Wang, and Y. Q. Tong, *Oral Surg. Oral Med. Oral Pathol. Oral Radiol. Endod* **108**, 368 (2009).
- ³⁶I. d. S. V. Marques, V. A. R. Barão, N. C. d. Cruz, J. C.-C. Yuan, M. F. Mesquita, A. P. Ricomini-Filho, C. Sukotjo, and M. T. Mathew, *Corros. Sci.* **100**, 133 (2015).
- ³⁷C. Vendemiatti, R. S. Hosokawa, R. C. C. Rangel, J. R. R. Bortoleto, N. C. Cruz, and E. C. Rangel, *Surf. Coatings Technol.* **275**, 32 (2015).
- ³⁸L. Muller and F. A. Muller, *Acta Biomater.* **2**, 181 (2006).
- ³⁹V. A. Barao, M. T. Mathew, J. C. Yuan, K. L. Knoernschild, W. G. Assunção, M. A. Wimmer, and C. Sukotjo, *J. Prosthet. Dent.* **110**, 462 (2013).
- ⁴⁰M. T. Mathew, V. A. Barao, J. C. Yuan, W. G. Assunção, C. Sukotjo, and M. A. Wimmer, *J. Mech. Behav. Biomed. Mater.* **8**, 71 (2012).
- ⁴¹I. d. S. V. Marques, N. C. d. Cruz, R. Landers, J. C.-C. Yuan, M. F. Mesquita, C. Sukotjo, M. T. Mathew, and V. A. R. Barão, *Biointerphases* **10**, 041002 (2015).
- ⁴²G. Ciobanu and O. Ciobanu, *Mater. Sci. Eng. C Mater. Biol. Appl.* **33**, 1683 (2013).
- ⁴³L. P. Faverani, W. G. Assunção, P. S. P. de Carvalho, J. C. C. Yuan, C. Sukotjo, M. T. Mathew, and V. A. Barao, *PLoS One* **9**, (2014).
- ⁴⁴W. G. Assunção, J. R. Jorge, P. H. Dos Santos, V. A. Barao, E. A. Gomes, and J. A. Delben, *J. Prosthodont.* **20**, 523 (2011).
- ⁴⁵E. C. Combe, B. A. Owen, and J. S. Hodges, *Dent. Mater.* **20**, 262 (2004).
- ⁴⁶H. H. Huang, Y. S. Sun, C. P. Wu, C. F. Liu, P. K. Liaw, and W. Kai, *Intermetallics* **30**, 139 (2012).
- ⁴⁷T. Fu, Z. Zhan, L. Zhang, Y. Yang, Z. Liu, J. Liu, L. Li, and X. Yu, *Surf. Coatings Technol.* **280**, 129 (2015).
- ⁴⁸V. Barranco, M. L. Escudero, M. C. Garcia-Alonso, *Electrochim. Acta* **52**, 4374 (2007).
- ⁴⁹L. Wen, Y. M. Wang, Y. Zhou, L. X. Guo, and J. H. Ouyang, *Corros. Sci.* **53**, 473 (2011).
- ⁵⁰S. Rossi, L. Fedrizzi, T. Bacci, and G. Pradelli, *Corros. Sci.* **45**, 511 (2003).
- ⁵¹M. Shokouhfar, C. Dehghanian, M. Montazeri, and A. Baradaran, *Appl. Surf. Sci.* **258**, 2416 (2012).
- ⁵²M. Babaei, C. Dehghanian, and M. Vanaki, *Appl. Surf. Sci.* **357**, 712 (2015).
- ⁵³B. Burnat, M. Walkowiak-Przybylo, T. Blaszczyk, and L. Klimek, *Acta Bioeng. Biomech.* **15**, 87 (2013).
- ⁵⁴E. Matykina, R. Arrabal, M. Mohedano, A. Pardo, M. C. Merino, and E. Rivero, *J. Mater. Sci. Mater. Med.* **24**, 37 (2013).
- ⁵⁵S. Cui, X. Yin, Q. Yu, Y. Liu, D. Wang, and F. Zhou, *Corros. Sci.* **98**, 471 (2015).
- ⁵⁶X. L. Zhu, K. H. Kim, and Y. S. Jeong, *Biomaterials* **22**, 2199 (2001).
- ⁵⁷L. Le Guehennec, A. Soueidan, P. Layrolle, and Y. Amouriq, *Dent. Mater.* **23**, 844 (2007).
- ⁵⁸T. Hayakawa, M. Yoshinari, and K. Nemoto, *Biomaterials* **25**, 119 (2004).
- ⁵⁹N. A. Krasteva, G. Toromanov, K. T. Hristova, E. I. Radeva, E. V. Pecheva, and R. P. Dimitrova, *J. Phys.: Conf. Ser.*, 012079 (2010).
- ⁶⁰C. A. Zamperini, L. Carneiro Hde, E. C. Rangel, N. C. Cruz, C. E. Vergani, and A. L. Machado, *Mycoses* **56**, 134 (2013).
- ⁶¹J. L. Xu, F. Liu, F. P. Wang, D. Z. Yu, and L. C. Zhao, *Appl. Surf. Sci.* **254**, 6642 (2008).
- ⁶²G. B. de Souza, G. G. de Lima, N. K. Kuromoto, P. Soares, C. M. Lepienski, C. E. Foerster, and A. Mikowski, *J. Mech. Behav. Biomed. Mater.* **4**, 796 (2011).
- ⁶³S. Durdu, O. F. Deniz, I. Kutbay, and M. Usta, *J. Alloys Compounds* **551**, 422 (2013).
- ⁶⁴M. S. Kim, J. J. Ryu, and Y. M. Sung, *Electrochem. Commun.* **9**, 1886 (2007).
- ⁶⁵N. E. Blanchard, B. Hanselmann, J. Drosten, M. Heuberger, and D. Hegemann, *Plasma Processes Polymers* **12**, 32 (2015).
- ⁶⁶I. Jouanny, S. Labdi, P. Aubert, C. Buscema, O. Maciejak, M. H. Berger, V. Guipont, and M. Jeandin, *Thin Solid Films* **518**, 3212 (2010).
- ⁶⁷S. Durdu, M. Usta, and A. S. Berkem, *Surf. Coatings Technol.*, in press (2015) doi:10.1016/j.surfcoat.2015.07.053.
- ⁶⁸A. Zareidoost, M. Yousefpour, B. Ghaseme, and A. Amanzadeh, *J. Mater. Sci.-Mater. Med.* **23**, 1479 (2012).

- ⁶⁹C. H. Yang, Y. T. Wang, W. F. Tsai, C. F. Ai, M. C. Lin, and H. H. Huang, *Clin. Oral Implants Res.* **22**, 1426 (2011).
- ⁷⁰O. Zywitzki, T. Modes, H. Sahm, P. Frach, K. Goedicke, and D. Gloss, *Surf. Coatings Technol.* **180**, 538 (2004).
- ⁷¹J. M. Wheeler, C. A. Collier, J. M. Paillard, and J. A. Curran, *Surf. Coatings Technol.* **204**, 3399 (2010).
- ⁷²T. Hara, K. Matsuoka, K. Matsuzaka, M. Yoshinari, and T. Inoue, *Bull. Tokyo Dent. Coll.* **53**, 45 (2012).
- ⁷³E. S. Thian, Z. Ahmad, J. Huang, M. J. Edirisinghe, S. N. Jayasinghe, D. C. Ireland, R. A. Brooks, N. Rushton, W. Bonfield, and S. M. Best, *Acta Biomater.* **6**, 750 (2010).
- ⁷⁴P. Parhi, A. Golas, and E. A. Vogler, *J. Adhes. Sci. Technol.* **24**, 853 (2010).
- ⁷⁵G. Mendonça, D. B. Mendonça, F. J. Aragão, and L. F. Cooper, *Biomaterials* **29**, 3822 (2008).
- ⁷⁶I. Han, B. Vagaska, B. J. Park, M. H. Lee, S. J. Lee, and J. C. Park, *J. Appl. Phys.* **109**, 124701 (2011).
- ⁷⁷Q. Yang, Y. Zhang, M. Liu, M. Ye, Y. Zhang, and S. Yao, *Anal. Chim. Acta* **597**, 58 (2007).
- ⁷⁸A. D. Roddick-Lanzilotta, P. A. Connor, and A. J. McQuillan, *Langmuir* **14**, 6479 (1998).
- ⁷⁹J. A. Lee and W. K. Lee, *J. Industrial Eng. Chem.* **19**, 1448 (2013).

Conclusão

No presente estudo, a síntese bem-sucedida de superfícies biofuncionais utilizando oxidação por plasma eletrolítico e plasma por descarga incandescente foi demonstrada. De acordo com nossos resultados, as superfícies tratadas com plasma foram capazes de melhorar o comportamento eletroquímico do Ticp quando comparadas às superfícies polidas e jateadas. Com relação às soluções eletrolíticas, a saliva artificial ácida reduziu a resistência à corrosão do Ticp. A presença de poros (aparência de vulcão) na superfície tratada com PEO foi notada através das imagens obtidas por MEV e AFM. Na superfície modificada por PEO não foi observada descontinuidade do filme e a camada de óxido formada apresentou espessura de aproximadamente 5 μm . Na superfície de Ticp tratada com PDI, foi formado um filme fino de 0,76 μm . O grupo do PEO mostrou a formação de estrutura cristalina na camada de óxido, com a presença de picos de rutilo e anatase. A presença de íons de Ca e P afetaram positivamente os resultados de adsorção de proteínas, principalmente de fibrinogênio, pois promoveu um maior número de sítios de ligação disponíveis para proteína. A superfície jateada também mostrou ótima adsorção de proteínas devido sua alta rugosidade de superfície. Dessa forma, são sugeridos estudos futuros para avaliar a interação de células e formação de osso sobre as superfícies tratadas com plasma e ainda, investigar o comportamento desses tratamentos quanto ao desgaste e corrosão (tribocorrosão) para entender o mecanismo de degradação no corpo humano. Além disso, estudos clínicos são necessários para avaliar a longevidade dos tratamentos propostos em implantes dentários e ortopédicos.

Referências¹

- Albrektsson T, Wennerberg A. Oral implant surfaces: Part 2--review focusing on clinical knowledge of different surfaces. *Int J Prosthodont*. 2004;17(5):544-64.
- Alves AC, Oliveira F, Wenger F, Ponthiaux P, Celis J-P, Rocha LA. Tribocorrosion behaviour of anodic treated titanium surfaces intended for dental implants. *J Physics D: Appl Physics*. 2013;46.
- Arima Y, Iwata H. Effect of wettability and surface functional groups on protein adsorption and cell adhesion using well-defined mixed self-assembled monolayers. *Biomater*. 2007;28(20):3074-82.
- Aronsson BO, Lausmaa J, Kasemo B. Glow discharge plasma treatment for surface cleaning and modification of metallic biomaterials. *J Biomed Mater Res*. 1997;35(1):49-73.
- Barao VA, Mathew MT, Assuncao WG, Yuan JC, Wimmer MA, Sukotjo C. Stability of cp-Ti and Ti-6Al-4V alloy for dental implants as a function of saliva pH - an electrochemical study. *Clin Oral Implants Res*. 2012;23(9):1055-62.
- Bassi F, Carr AB, Chang TL, Estafanous E, Garrett NR, Happonen RP, et al. Clinical outcomes measures for assessment of longevity in the dental implant literature: ORONet approach. *Int J Prosthodont*. 2013;26(4):323-30.
- Bazaka K, Jacob MV, Crawford RJ, Ivanova EP. Plasma-assisted surface modification of organic biopolymers to prevent bacterial attachment. *Acta Biomater*. 2011;7(5):2015-28.
- Bergkvist M, Carlsson J, Oscarsson S. Surface-dependent conformations of human plasma fibronectin adsorbed to silica, mica, and hydrophobic surfaces, studied with use of Atomic Force Microscopy. *J Biomed Mater Res A*. 2003;64(2):349-56.
- Bordji K, Jouzeau JY, Mainard D, Payan E, Netter P, Rie KT, et al. Cytocompatibility of Ti-6Al-4V and Ti-5Al-2.5Fe alloys according to three surface treatments, using human fibroblasts and osteoblasts. *Biomater*. 1996;17(9):929-40.
- Chang Y-C, Feng S-W, Huang H-M, Teng N-C, Lin C-T, Lin H-K, et al. Surface Analysis of Titanium Biological Modification with Glow Discharge. *Clin Implant Dent Relat Res*. 2013;17(3):469-75.
- Coelho PG, de Assis SL, Costa I, Thompson VP. Corrosion resistance evaluation of a Ca- and P-based bioceramic thin coating in Ti-6Al-4V. *J Mater Sci Mater Med*. 2009;20(1):215-22.
- Correa CB, Pires JR, Fernandes-Filho RB, Sartori R, Vaz LG. Fatigue and fluoride corrosion on *Streptococcus mutans* adherence to titanium-based implant/component surfaces. *J Prosthodont*. 2009;18(5):382-7.
- Cortada M, Giner L, Costa S, Gil FJ, Rodriguez D, Planell JA. Galvanic corrosion behavior of titanium implants coupled to dental alloys. *J Mater Sci Mater Med*. 2000;11(5):287-93.

¹ De acordo com as normas da UNICAMP/FOP, baseadas na padronização do International Committee of Medical Journal Editors. Abreviatura dos periódicos em conformidade com o Medline

- Czarnowska E, Wierzchon T, Maranda-Niedbala A, Karczmarewicz E. Improvement of titanium alloy for biomedical applications by nitriding and carbonitriding processes under glow discharge conditions. *J Mater Sci Mater Med*. 2000;11(2):73-81.
- Davies JE. Understanding peri-implant endosseous healing. *J Dent Educ*. 2003;67(8):932-49. Epub 2003/09/10.
- Dong YM, Pearce EI, Yue L, Larsen MJ, Gao XJ, Wang JD. Plaque pH and associated parameters in relation to caries. *Caries Res*. 1999;33(6):428-36.
- Edgarg M, Dawes C, O'Mullane D. *Saliva e Saúde Bucal - Composição, função e efeitos protetores*. 3 ed.- São Paulo. Santos, 2010. 46p.
- Eisenbarth E, Velten D, Muller M, Thull R, Breme J. Biocompatibility of beta-stabilizing elements of titanium alloys. *Biomater*. 2004;25(26):5705-13.
- Felgueiras HP, Castanheira L, Changotade S, Poirier F, Oughlis S, Henriques M, et al. Biotribocorrosion (tribo-electrochemical) characterization of anodized titanium biomaterial containing calcium and phosphorus before and after osteoblastic cell culture. *J Biomed Mater Res Part B: Appl Biomater*. 2014;103(3):661-9.
- Flatebo RS, Hol PJ, Leknes KN, Kosler J, Lie SA, Gjerdet NR. Mapping of titanium particles in peri-implant oral mucosa by laser ablation inductively coupled plasma mass spectrometry and high-resolution optical darkfield microscopy. *J Oral Pathol Med*. 2011;40(5):412-20.
- Gao L, Feng B, Wang J, Lu X, Liu D, Qu S, et al. Micro/nanostructural porous surface on titanium and bioactivity. *J Biomed Mater Res B Appl Biomater*. 2009;89(2):335-41.
- Gittens RA, Olivares-Navarrete R, Tannenbaum R, Boyan BD, Schwartz Z. Electrical implications of corrosion for osseointegration of titanium implants. *J Dent Res*. 2011;90(12):1389-97.
- Gregory-Head BL, Curtis DA, Kim L, Cello J. Evaluation of dental erosion in patients with gastroesophageal reflux disease. *J Prosthet Dent*. 2000;83(6):675-80.
- Guindy JS, Schiel H, Schmidli F, Wirz J. Corrosion at the marginal gap of implant-supported suprastructures and implant failure. *Int J Oral Maxillofac Implants*. 2004;19(6):826-31.
- Hanawa T, Kaga M, Itoh Y, Echizenya T, Oguchi H, Ota M. Cytotoxicities of oxides, phosphates and sulphides of metals. *Biomater*. 1992;13(1):20-4.
- Hanawa T. A comprehensive review of techniques for biofunctionalization of titanium. *J Periodontal Implant Sci*. 2011;41(6):263-72.
- Hao L, Lawrence J. On the role of CO₂ laser treatment in the human serum albumin and human plasma fibronectin adsorption on zirconia (MGO-PSZ) bioceramic surface. *J Biomed Mater Res A*. 2004;69(4):748-56.

- Hauser J, Zietlow J, Koller M, Esenwein SA, Halfmann H, Awakowicz P, et al. Enhanced cell adhesion to silicone implant material through plasma surface modification. *J Mater Sci Mater Med*. 2009;20(12):2541-8.
- Huang YH, Xiropaidis AV, Sorensen RG, Albandar JM, Hall J, Wikesjo UM. Bone formation at titanium porous oxide (TiUnite) oral implants in type IV bone. *Clin Oral Implants Res*. 2005;16(1):105-11.
- Jacobs JJ, Skipor AK, Patterson LM, Hallab NJ, Paprosky WG, Black J, et al. Metal release in patients who have had a primary total hip arthroplasty. A prospective, controlled, longitudinal study. *J Bone Joint Surg Am*. 1998;80(10):1447-58.
- Janocha B, Hegemann D, Oehr C, Brunner H, Rupp F, Geis-Gerstorfer J. Adsorption of protein on plasma-polysiloxane layers of different surface energies. *Surf Coat Technol*. 2001;142:1051-5.
- Joska L, Fojt J, Hradilova M, Hnilica F, Cvrcek L. Corrosion behaviour of TiN and ZrN in the environment containing fluoride ions. *Biomed Mater*. 2010;5(5):054108.
- Kibayashi H, Teraoka F, Fujimoto S, Nakagawa M, Takahashi J. Surface modification of pure titanium by plasma exposure and its bonding to resin. *Dent Mater J*. 2005;24(1):53-8.
- Kilpadi KL, Chang PL, Bellis SL. Hydroxylapatite binds more serum proteins, purified integrins, and osteoblast precursor cells than titanium or steel. *J Biomed Mater Res*. 2001;57(2):258-67.
- Kotsovilis S, Karoussis IK, Fourmouis I. A comprehensive and critical review of dental implant placement in diabetic animals and patients. *Clin Oral Implants Res*. 2006;17(5):587-99.
- Lee SH, Lee DC. Preparation and characterization of thin films by plasma polymerization of hexamethyldisiloxane. *Thin Solid Films*. 1998;325(1-2):83-6.
- Li Y, Zou S, Wang D, Feng G, Bao C, Hu J. The effect of hydrofluoric acid treatment on titanium implant osseointegration in ovariectomized rats. *Biomater*. 2010;31(12):3266-73.
- Lopes B, Rangel R, Antonio C, Durrant S, Cruz N, Rangel E (2012). Mechanical and Tribological Properties of Plasma Deposited a-C:H:Si:O Films. Chapter 8. In: Nemecek J. Nanoindentation in Materials Science. Intech. doi: 10.5772/50278.
- Mabboux F, Ponsonnet L, Morrier JJ, Jaffrezic N, Barsotti O. Surface free energy and bacterial retention to saliva-coated dental implant materials--an in vitro study. *Colloids Surf B Biointerfaces*. 2004;39(4):199-205.
- MacDonald DE, Rapuano BE, Vyas P, Lane JM, Meyers K, Wright T. Heat and radiofrequency plasma glow discharge pretreatment of a titanium alloy promote bone formation and osseointegration. *J Cell Biochem*. 2013;114(10):2363-74.
- Matthew IR, Frame JW, Browne RM, Millar BG. In vivo surface analysis of titanium and stainless steel miniplates and screws. *Int J Oral Maxillofac Surg*. 1996;25(6):463-8.

- Messer RL, Seta F, Mickalonis J, Brown Y, Lewis JB, Wataha JC. Corrosion of phosphate-enriched titanium oxide surface dental implants (TiUnite) under in vitro inflammatory and hyperglycemic conditions. *J Biomed Mater Res B Appl Biomater*. 2010;92(2):525-34.
- Murrell S, Marshall TA, Moynihan PJ, Qian F, Wefel JS. Comparison of in vitro erosion potentials between beverages available in the United Kingdom and the United States. *J Dent*. 2010;38(4):284-9.
- Nakagawa M, Matsuya S, Udoh K. Effects of fluoride and dissolved oxygen concentrations on the corrosion behavior of pure titanium and titanium alloys. *Dent Mater J*. 2002;21(2):83-92.
- Nikolopoulou F. Saliva and dental implants. *Implant Dent*. 2006;15(4):372-6. Epub 2006/12/19.
- Olmedo D, Guglielmotti MB, Cabrini RL. An experimental study of the dissemination of Titanium and Zirconium in the body. *J Mater Sci Mater Med*. 2002;13(8):793-6.
- Olmedo DG, Paparella ML, Brandizzi D, Cabrini RL. Reactive lesions of peri-implant mucosa associated with titanium dental implants: a report of 2 cases. *Int J Oral Maxillofac Surg*. 2010;39(5):503-7.
- Olmedo DG, Paparella ML, Spielberg M, Brandizzi D, Guglielmotti MB, Cabrini RL. Oral mucosa tissue response to titanium cover screws. *J Periodontol*. 2012;83(8):973-80.
- Rafieerad AR, Ashra MR, Mahmoodian R, Bushroa AR. Surface characterization and corrosion behavior of calcium phosphate-base composite layer on titanium and its alloys via plasma electrolytic oxidation: A review paper. *Mater Sci Eng C* 2015;57:397–413
- Rapuano BE, Hackshaw KM, Schniepp HC, MacDonald DE. Effects of Coating a Titanium Alloy with Fibronectin on the Expression of Osteoblast Gene Markers in the MC3T3 Osteoprogenitor Cell Line. *Int J Oral Maxillofac Implants*. 2012;27(5):1081-90.
- Sawase T, Jimbo R, Wennerberg A, Suketa N, Tanaka Y, Atsuta M. A novel characteristic of porous titanium oxide implants. *Clin Oral Implants Res*. 2007;18(6):680-5.
- Schiff N, Grosogeat B, Lissac M, Dalard F. Influence of fluoride content and pH on the corrosion resistance of titanium and its alloys. *Biomater*. 2002;23(9):1995-2002.
- Schropp L, Wenzel A, Stavropoulos A. Early, delayed, or late single implant placement: 10-year results from a randomized controlled clinical trial. *Clin Oral Implants Res*. 2014;25:1359–65.
- Sharma CP, Hari PR. Adhesion and stability of blood cells onto polymer substrates: effect of glow discharge. *J Biomater Appl*. 1991;6(1):72-9.
- Souza JC, Ponthiaux P, Henriques M, Oliveira R, Teughels W, Celis JP, et al. Corrosion behaviour of titanium in the presence of *Streptococcus mutans*. *J Dent*. 2013;41(6):528-34.
- Souza JCM, Henriques M, Teughels W, Ponthiaux P, Celis J-P, Rocha LA. Wear and Corrosion Interactions on Titanium in Oral Environment: Literature Review. *J of Bio and Tribo Corr*. 2015.

- Urban RM, Jacobs JJ, Tomlinson MJ, Gavrilovic J, Black J, Peoc'h M. Dissemination of wear particles to the liver, spleen, and abdominal lymph nodes of patients with hip or knee replacement. *J Bone Joint Surg Am*. 2000;82(4):457-76.
- Vargas E, Baier RE, Meyer AE. Reduced corrosion of CP Ti and Ti-6Al-4V alloy endosseous dental implants after glow-discharge treatment: a preliminary report. *Int J Oral Maxillofac Implants*. 1992;7(3):338-44.
- Vieira AC, Ribeiro AR, Rocha LA, Celis JP. Influence of pH and corrosion inhibitors on the tribocorrosion of titanium in artificial saliva. *Wear*. 2006;261(9):994-1001.
- Yun KD, Yang YZ, Lim HP, Oh GJ, Koh JT, Bae IH, et al. Effect of nanotubular-micro-roughened titanium surface on cell response in vitro and osseointegration in vivo. *Mater Sci Eng C Mater Biol Appl*. 2010;30(1):27-33.

Anexo 1 - (Copyright)

De: Nancy Schultheis <Nancy@ivst.org>
 Data: 20 de abril de 2016 13:27:04 BRT
 Para: Valentin Barao <ricardo.barao@hotmail.com>
 Cc: "ybarao@unicamp.br" <ybarao@unicamp.br>, "AIPRights Permissions (Rights@aip.org)" <Rights@aip.org>
 Assunto: RE: License to publish - Biointerphases

Dear Dr. Barao,

Thank you so much for your articles in *Biointerphases*! An author is permitted to include their published material in their thesis/dissertation, provided they credit the material appropriately and acknowledge the AVS' copyright. Our preferred statement is as follows:

"Reprinted with permission from [FULL CITATION]. Copyright [PUBLICATION YEAR], American Vacuum Society."

Full citation format is as follows: Author names, journal title, Vol. #, Page #, (Year of publication).

For an article, the copyright notice must be printed on the first page of the article or book chapter. For figures, photographs, covers, or tables, the notice may appear with the material, in a footnote, or in the reference list.

Please let us know if you have any questions. If you need a formal permission grant that includes specific language, please send a request directly to rights@aip.org.

Thank you again,

Nancy



*Science and Technology
of Materials, Interfaces, and Processing*

Nancy Schultheis
 AVS Publications Office Manager
 51 Kilmayne Drive, Suite 104
 Cary, NC 27511
 Phone: [919-361-2787](tel:919-361-2787)
 Cell: [919-884-6598](tel:919-884-6598)
 Fax: [919-234-0051](tel:919-234-0051)
nancy@ivst.org
 AVS Digital Library